viruses

MDPI

Article

Regions of Bovine Adenovirus-3 Protein VII Involved in Interactions with Viral and Cellular Proteins

Shermila Kulanayake [1,2], Faryal Dar [1,2] and Suresh K. Tikoo [1,2,3,*]

[1] Vaccinology & Immunotherapeutics Program, School of Public Health, University of Saskatchewan, Saskatoon, SK S7N 5E5, Canada; shermila.kulanayake@usask.ca (S.K.); uyl039@mail.usask.ca (F.D.)
[2] Vaccine and Infectious Disease Organization (VIDO), University of Saskatchewan, Saskatoon, SK S7N 5E5, Canada
[3] Veterinary Microbiology, Western College of Veterinary Medicine, University of Saskatchewan, Saskatoon, SK S7N 5B4, Canada
* Correspondence: suresh.tik@usask.ca

Abstract: The L 1 region of bovine adenovirus (BAdV)-3 encodes a multifunctional protein named protein VII. Anti-protein VII sera detected a protein of 26 kDa in transfected or BAdV-3-infected cells, which localizes to nucleus and nucleolus of infected/transfected cells. Analysis of mutant protein VII identified four redundant overlapping nuclear/nucleolar localization signals as deletion of all four potential nuclear/nucleolar localization signals localizes protein VII predominantly to the cytoplasm. The nuclear import of protein VII appears to use importin α (α-1), importin-β (β-1) and transportin-3 nuclear transport receptors. In addition, different nuclear transport receptors also require part of protein VII outside nuclear localization sequences for efficient interaction. Proteomic analysis of protein complexes purified from recombinant BAdV-3 expressing protein VII containing Strep Tag II identified potential viral and cellular proteins interacting with protein VII. Here, we confirm that protein VII interacts with IVa2 and protein VIII in BAdV-3-infected cells. Moreover, amino acids 91–101 and 126–137, parts of non-conserved region of protein VII, are required for interaction with IVa2 and protein VIII, respectively.

Keywords: BAdV-3; protein VII; Importins; NLS/NoLS; protein–protein interactions

Citation: Kulanayake, S.; Dar, F.; Tikoo, S.K. Regions of Bovine Adenovirus-3 Protein VII Involved in Interactions with Viral and Cellular Proteins. *Viruses* **2024**, *16*, 732. https://doi.org/10.3390/v16050732

Academic Editor: Joe S. Mymryk

Received: 21 March 2024
Revised: 30 April 2024
Accepted: 30 April 2024
Published: 5 May 2024

1. Introduction

Bovine adenovirus (BAdV)-3 is a non-enveloped, double-stranded DNA virus which belongs to *Mastadenovirus* genus. The genome is 34446bp in length and can be divided into early, intermediate and late regions [1]. The inner core (genome, protein VII, protein V, protein IVa2, protein X, protease and terminal protein) and the outer capsid (hexon, penton base and fiber) of the icosahedral virus are connected by four cementing proteins named protein IIIa, protein VI, protein VIII and protein IX, which are organized into two distinct layers [2].

Production of progeny adenovirus requires proteins encoded by intermediate and late region of members of *Mastadenovirus* genus to localize from the cytoplasm to nucleus/nucleolus of infected cells [3]. While most adenovirus proteins contain motifs required to localize the protein to nucleus [3–5], some adenovirus proteins utilize and interact with other adenovirus proteins to localize to the nucleus [6]. Irrespective of the mode of nuclear transport of adenoviral proteins, specific motifs called nuclear localization signals (NLSs) present in these proteins need to interact with importin and/or transportin-3 receptors before passing through the nuclear pore complex (NPC) [5–7]. In contrast, the nucleolar transport of viral protein requires retention of viral protein in the nucleolus by interaction of undefined motifs of proteins designated nucleolar localization signals (NoLSs) with resident nucleolar protein or RNA [8].

Adenovirus protein VII, a most abundant core protein encoded by late region [1] of the genome, acts as a functional analog of the cellular histone [9,10]. Moreover, interaction of protein VII with viral and cellular proteins facilitates the involvement of protein VII in different aspects of the adenovirus–host interaction [11]. Although protein VII appeared to be involved in condensing genomic DNA into the virion [12,13], a recent report suggests that protein VII is not required for condensing genomic DNA into capsids [14].

While location of proteins encoded by members of *Mastadenovirus* genus appears conserved [15], recent reports suggest that structure and function of many homologous proteins encoded by members of *Mastadenovirus* genus may not be conserved [3,16–18]. Interestingly, BAdV-3 protein VII shows 39–45% homology with protein VII encoded by other members of *Mastadenovirus* genus. Since BAdV-3 protein VII shows lower degree of homology, we characterized BAdV-3 protein VII. Here, we report the subcellular localization and stable interactions of BAdV-3 protein VII with other viral and cellular proteins which may play important roles in BAdV-3 life cycle.

2. Materials and Methods

2.1. Cell Lines and Viruses

Madin–Darby bovine kidney (MDBK) (ATCC CCL22), cotton rat lung fibroblast (CRL; [19]) and VIDO DT1 (cotton rat lung fibroblast [19] expressing endonuclease *I-SceI*) [20]) cells were propagated at 37 °C and 5% CO_2 in minimal essential medium (MEM; Sigma, Tokyo, Japan). The Human embryo kidney (HEK 293T) (ATCC CRL-11268) and African green monkey kidney (Vero) (ATCC CCL-81) cells were propagated in Dulbecco's modified minimal essential medium (DMEM; Sigma). All media were supplemented with heat-inactivated 10% fetal bovine serum (FBS; SAFC industries, Sigma), 10 mM HEPES (Gibco), 0.1 mM nonessential amino acids (NEAA; Gibco), and 50 µg/mL gentamicin (Bio Basics). MDBK and CRL cells (only non-bovine cells) are used mainly for growing bovine adenoviruses. Due to high transfection efficiency, HEK293T cells are used for Western blots. Vero cells are usually used for sub-cellular localization as these cells have a distinct nucleus and a cytoplasm. VIDO DT1 cells are used for generating recombinant BAdV-3. Yeast S288c cells was a gift from Dr. Troy Harkness, University of Saskatchewan, Canada. Wild-type BAdV-3, BAV304a (E3 region replaced with EYFP [expressing enhanced yellow fluorescent protein] under CMV promoter) [20] and recombinant BAV.VII.Strep (this study) was propagated in MDBK cells [1] in MEM supplemented with 2% fetal bovine serum.

2.2. Antibodies

Anti-HA mouse monoclonal antibody (A1978), anti-nucleolin rabbit polyclonal antibody (N2662), anti -nucleolin mouse monoclonal antibody (SAB1305550) and anti-β-Actin mouse monoclonal antibody (H9658) were purchased from Sigma, Canada. Alexa 488-conjugated goat anti-mouse antibody (catalog #115-545-003) was purchased from Invitrogen, Burlington, ON, Canada. FITC-conjugated goat anti-rabbit antibody, FITC-conjugated goat anti-mouse, alkaline phosphatase (AP)-conjugated goat anti-rabbit IgG, alkaline phosphatase (AP)-conjugated goat anti-mouse IgG, TRITC-conjugated goat anti-rabbit antibody and TRITC-conjugated goat anti-mouse were purchased from Jackson Immune Research. Production and characterization of antibodies against BAdV-3 protein VII [21], DNA binding protein (DBP) [22], protein VIII [23] and protein IVa2 [5] have been described previously.

2.3. Plasmid Construction

Plasmid pC.HA (plasmid pcDNA3 containing 3HA tag) was provided by Dr. Joyce Wilson, University of Saskatchewan, Canada. Plasmid pGC.linker and pGN.linker were gifted by Dr. Abraham Loyter, Hebrew University, Jerusalem, Israel. The plasmids encoding GST-fused importin α-1, importin α-3, importin α-5, importin α-7 and importin β-were kindly provided by M. Kohler and have been described [24]. Plasmid-expressing GST-importin α-9-fused protein was kindly provided by Dr. Yuh Min Chook, UT Southwestern Medical Center, Dallas, USA. Plasmid-expressing GST-fused importin α-11 was

kindly provided by Dr. Scott M. Plafker, Oklahoma Medical Research Foundation (OMRF), Oklahoma City, OK, USA. Plasmid-expressing GST importin 13 was provided by Dr. David Jans, Biomedicine Discovery Institute, Monash University, Clayton, VIC, Australia. Plasmid pGST-TRN-SR2 was a gift from Dr. Woan-Yuh Tarn and has been described [25]. Plasmid pRSETnucleolin was purchased from Addgene.

The details of the construction of other plasmids used in this study are depicted in Supplementary File.

2.4. Transfection

293T or VIDO DT1 cells were transfected with individual plasmid DNA (5 μg/10^6 cells) using Lipofectamine TM 2000 (Invitrogen) as per manufacturer's instructions. After 4–6 h post transfection, the transfection medium was replaced with fresh medium containing 2% FBS, and the cells were incubated for indicated times for further analysis.

2.5. Western Blotting

Proteins from the lysates of the cells infected with virus or transfected with plasmid DNA were detected by Western blotting as described [26] using protein-specific antiserum and alkaline phosphatase-conjugated secondary antibodies.

2.6. Indirect Immunofluorescence Assay

Virus-infected or plasmid DNA-transfected cells were fixed with 3.7% paraformaldehyde for 15 min before permeabilizing with 0.5% Triton X-100 followed by blocking with 5% FBS. After blocking the cells with 5% FBS for 60 min, the cells were incubated with protein-specific primary antibody followed by fluorophore-conjugated secondary antibodies. Finally, the cells were mounted with mounting medium (VectaShield) containing 4′, 6-diamidino-2-phenylindole (DAPI) and imaged under Zeiss LSM 5 Laser scanning confocal microscope.

2.7. GST Pull-Down Assay

GST fusion proteins (Importin α1, α3, α5, α7, α9, α11, α13, β1 and transportin-3) were purified from *E. coli* BL21 transformed with individual plasmid DNA by glutathione Sepharose beads (Cytiva, Marlborough, USA). Individual purified proteins were mixed with the lysate of 293T cells transfected with plasmid pC.HA.VII DNAs. After a 2 h incubation, the beads with the attached protein complexes were pulled down by centrifugation, washed extensively and analyzed by Western blot using anti-HA MAb.

2.8. Bimolecular Fluorescence Complementation (BiFC) Analysis

The BiFC assay was performed as described earlier [27]. Briefly, the competent yeast cells were co-transfected with indicated plasmid DNAs according to the polyethylene glycol –Lithium acetate (PEG-LiAc) method (Clontech Laboratories 2009). Co-transformed cells were plated on to a selective drop-out medium supplemented with 2% glucose in the absence of urease and histidine and incubated at 30 °C for 3–5 days. Finally, the colonies were picked, spread and fixed on slides, mounted with a mounting medium containing DAPI (Vectashield) and examined using a Zeiss LSM 5 laser scanning confocal microscope.

2.9. Isolation of Recombinant BAdV-3 (BAV.VII.ST)

Recombinant BAdV-3-expressing protein VII containing Strep Tag was isolated as described [28]. The monolayer of VIDO DT1 cells in a six-well plate was transfected with 2–4 μg of plasmid pUC304a.VII.Strep DNA using Lipofectamine 2000 reagent (Invitrogen). At 4–6 h post transfection, the medium was replaced with fresh MEM containing 2% FBS. The cells were observed daily for cytopathic effect (CPE). Once CPE developed, the cells were harvested, freeze-thawed three times and propagated in MDBK cells. The recombinant was designated as BAV.VII.ST.

2.10. Virus Growth

Monolayers of MDBK cells in 24-well plates were infected with wild-type or recombinant BAdV-3 at MOI of 5. After adsorption for 2 h at 37 °C, the inoculum was removed and the cells were incubated in a fresh medium containing 2% FBS. At indicated times post infection, the infected cells were harvested, freeze-thawed three times and centrifuged at 3500 rpm for 5 min at 4 °C. Finally, the supernatant was collected and used to infect fresh monolayers of MDBK cells in triplicate. The cells were observed for fluorescent focus forming units and the titer was expressed as FFU/mL as described [26].

2.11. Purification and Identification of the Strep-Tagged Protein Complex

Strep-Tagged protein complexes were identified as described earlier [28]. Briefly, MDBK cells infected with BAV304a [20] or BAV.pVII.ST at a MOI of 5 were collected at 32 and 48 h post infection. The cells were washed with PBS and lysed with a cell lysis buffer (cell signaling technologies) supplemented with phenylmethylsulfonyl fluoride (PMSF). The cell lysates were centrifuged at 14,000× *g* for 15 min at 4 °C and supernatants were used to purify the Strep-Tagged protein complex using Strep-tactin sepharose according to the manufacturer's instruction. Briefly, the prewashed strep-tactin sepharose with buffer W (100 mM Tris-Cl, pH 8.0, 150 mM NaCl, 1 mM EDTA) was incubated with the supernatant at 4 °C. After overnight incubation, the lysate–sepharose mixture was drained to a polyprolene column. Non-specifically bound proteins were washed off with buffer W. Finally, the proteins attached to the sepharose beads were eluted with buffer E (buffer W containing 2.5 mM desthiobiotin), concentrated with an MWCO 10 kDa centrifugal filter (Millipore). The proteins in the Strep-Tagged protein VII complex were separated by SDS-PAGE and detected by silver staining. Finally, the protein in the complexes was identified by LC-MS/MS analysis at University of Victoria-Genome BC Proteomics Centre.

2.12. Co-Immunoprecipitation (Co-IP) Assay

MDBK or 293T cells infected with BAV304a [20] or co-transfected with indicated plasmid DNAs, collected after 48 h post infection/transfection, were lysed with a lysis buffer. The proteins from the lysates were incubated with indicated protein specific antibodies before protein complexes were precipitated using protein A-agarose (Thermo-Scientific, Irwindale, CA, USA). After 12 h of incubation at 4 °C, the immune complexes were washed with PBS to remove non-specific bindings. Finally, the proteins in the immune complexes were separated by 12% SDS-PAGE, which was analyzed by Western blotting using indicated protein-specific antibodies as described [29].

3. Results

3.1. Sequence Analysis of BAdV-3 Protein VII

First, homology between protein VII encoded by members of *Mastadenovirus* was analysed using the Clustalw program. As seen in Figure 1, compared to middle and C-terminus of protein VII, N-terminus shows higher degree of homology. Second, analysis of BAdV-3 protein VII by NLS mapper [30] and SBC software predicted the potential nuclear localization signals (NLS) located at amino acids 84–89, amino acids 95–99, amino acids 113–121 and amino acids 142–145 (Figure 1). Finally, predict protein software [31] was used to identify (between amino acids 52–53 of protein VII) the potential site (characteristics: hydrophilic region, not a potential protein binding site, disordered region) for insertion of Strep tag II motif (WSHPQFEK).

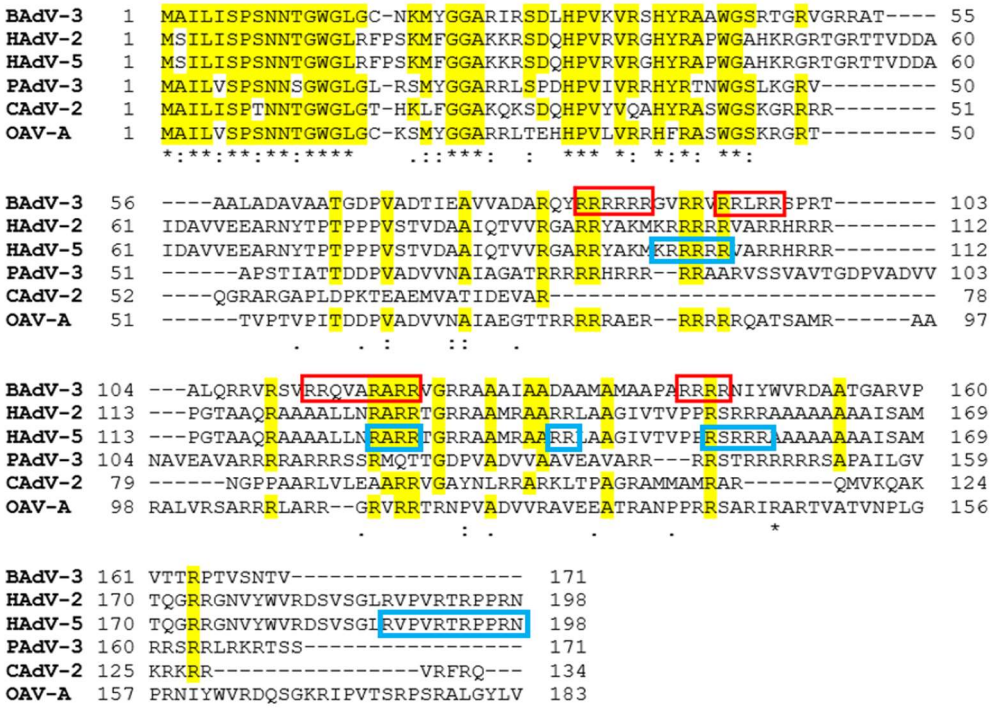

Figure 1. Analysis of BAdV-3 protein VII amino acid sequence homology. Alignment of amino acid sequences of protein VII of BAdV-3 (Genbank accession #NP0463119), HAdV-2 (Genbank accession # AP_000171.1), HAdV-5 (Genbank accession # AP000207.1), porcine adenovirus (PAdV)-3 (Genbank accession # YP_0098206.1) Canine adenovirus (CAdV)2 (Genbank accession # AP_000618.1), and Ovine adenovirus (OAV)-A (AP 000010.1). The identical amino acids are marked by (*) and shown in yellow color. The conserved amino acids are shown by (:). Predicted NLS are shown by box. BAdV-3 (red box); HAdV-5 (sky blue box).

3.2. Characterization of Protein VII

The cells infected with virus or transfected with indicated plasmid DNA (Figure 2A) were analyzed by Western blot using anti-VII sera [21] or anti-HA MAb. As seen in Figure 2B, anti-VII sera detected a protein of 26 kDa in BAdV-3-infected cells. No such protein could be detected in mock-infected cells. Similarly, anti-HA MAb detected a protein of 26 kDa in cells transfected with plasmid pC.HA.VII DNA. No such protein could be detected in plasmid pcDNA.3HA DNA-transfected cells.

To assess the subcellular localization of protein VII, infected or plasmid DNA transfected cells were analyzed 48 hr post infection/transfection by indirect immunofluorescence using anti-pVII serum or anti-HA MAb. As seen in Figure 2C, protein VII expressed in BAdV-3-infected (Panels a–c) or plasmid pC.HA.VII DNA-transfected cells localized in the nuclei (Panels d–f) of the cells. No such fluorescence could be detected in mock-infected cells (Panels g–i).

To determine whether protein VII is actively transported to the nucleus, subcellular localization of fusion protein VII-GFP-β-gal (amino acids 1–171 of BAdV-3 protein VII fused to N-terminus of cytoplasmic fusion protein GFP.β-gal [32]) was analyzed by direct fluorescence. As expected, the GFP.β-gal protein localized to the cytoplasm (Figure 2E, Panels d–f) of plasmid pGFP.β-gal DNA (Figure 2D)-transfected cells. Interestingly, fusion protein VII-GFP-β-gal localized to the nucleus of cells (Figure 2E, Panels g–i) transfected with plasmid pVII-GFP-β-gal (Figure 2D) DNA.

Moreover, fluorescent signals for protein VII and nucleolin coincide in the cells (Figure 2F, Panels a–d) transfected with plasmid pC.HA.VII DNA (Figure 2A) or cells infected with BAdV-3 (Figure 2F, Panels e–h).

The percentage of cells showing similar display of protein distribution is summarized in Supplementary File (Table S10).

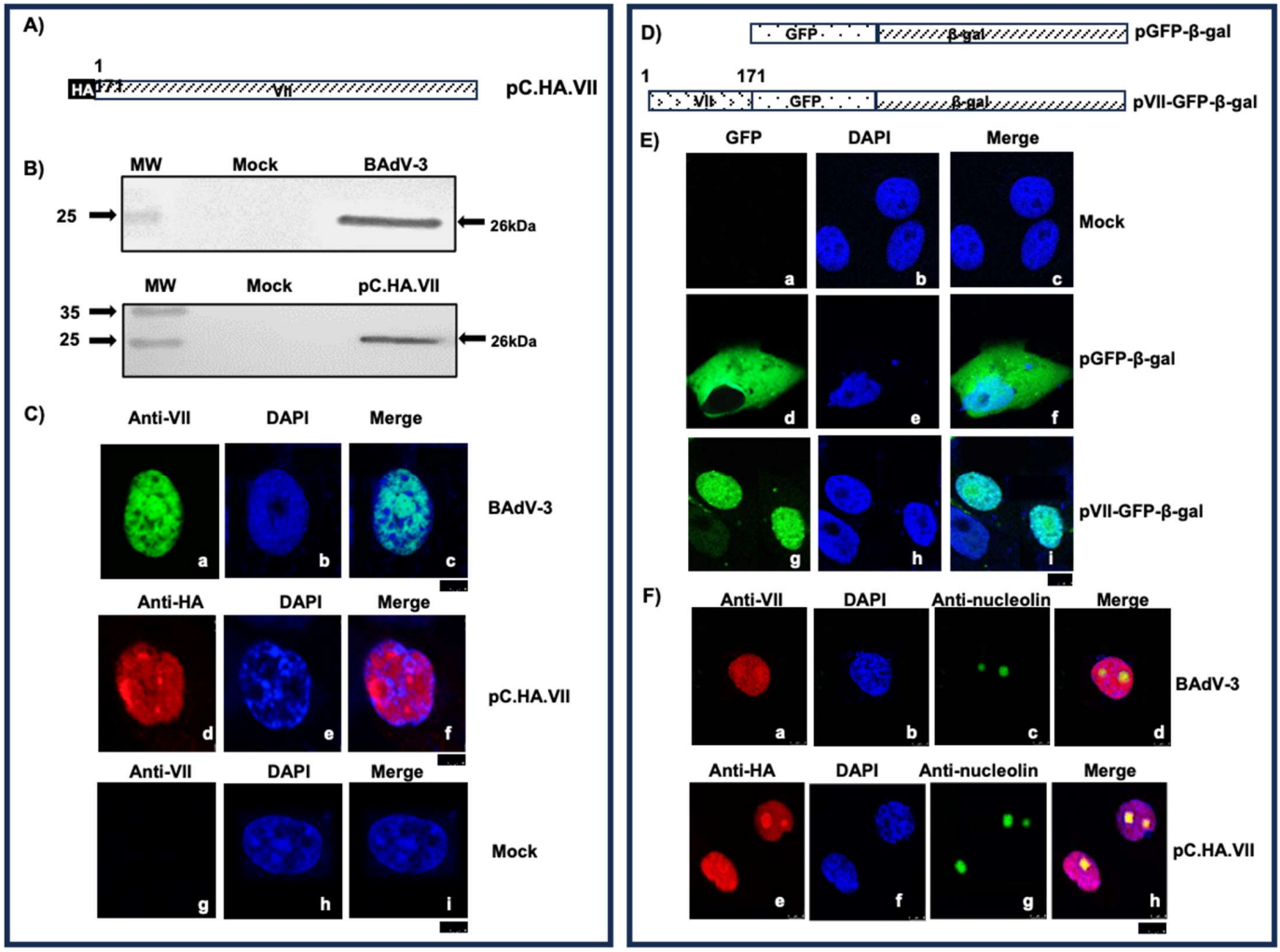

Figure 2. Expression of BAdV-3 protein VII. (**A**). Schematic diagram of proteins encoded by plasmid DNA. Amino acid numbers are depicted. The name of the plasmid is shown on the right of the panel. Hemagglutinin Tag (HA). (**B**). Western blot. Proteins from the lysates of BAdV-3-infected cells or plasmid pC.HA.VII DNA-transfected cells were separated by 12% SDS-PAGE, transferred to nitrocellulose and probed in Western blot using anti-pVII sera or anti-HA MAb. Molecular weight markers (MW), mock (uninfected/untransfected cells). (**C**–**F**). Sub-cellular localization of protein VII. (**C**). Nuclear localization of protein VII**.** CRL cells were infected with BAdV-3 (Panels a–c). After 48 h post infection, the cells were fixed with 3.7% formaldehyde and 0.2% TritonX-100. The location of protein VII was analyzed by indirect fluorescence using anti-VII serum [21]. The nuclei were stained with DAPI. Vero cells were transfected with plasmid pC.HA.VII DNA (Panels d–f). After 48 h post transfection, the cells were fixed with 3.7% formaldehyde and 0.2% TritonX-100. The location of protein VII was analyzed by indirect fluorescence using anti-HA MAb. The nuclei were stained with DAPI. The scale bar (3 μm) is shown as a black box. (**D**). Schematic diagram of proteins encoded by plasmid DNA. Amino acid numbers are depicted. The name of the plasmid is shown on the right of the panel. (**E**). Subcellular localization of VII-GFP-β-gal fusion protein. Vero cells were transfected with plasmid pGFP-β-gal DNA (Panels d–f) or plasmid pVII-GFP-β-gal DNA (Panels g–i). After 48 h post transfection, the cells were fixed with 3.7% formaldehyde and 0.2% TritonX-100. The location of fusion protein VII-GFP-β-gal was analyzed by direct fluorescence. The scale bar (5 μm) is shown as a black box (**F**). Nucleolar localization of protein VII. Vero cells transfected with plasmid pC.HA.VII DNA (Panels a–d). After 48 h post transfection, the cells were fixed with 3.7% formaldehyde and 0.2% TritonX-100 and analyzed using anti-HA MAb and anti-nucleolin rabbit sera followed by TRITC-conjugated goat anti-mouse IgG and

FITC-conjugated goat anti-rabbit IgG using confocal microscope TCS SP5 (Leica). CRL cells were infected with BAdV-3 (panels e–h). After 48 h post infection, the cells were fixed with 3.7% formaldehyde and 0.2% TritonX-100 and analyzed by indirect immunofluorescence using anti-pVII sera and anti-nucleolin MAb followed by TRITC-conjugated goat anti-rabbit IgG and FITC-conjugated goat anti-mouse IgG using confocal microscope TCS SP5 (Leica). The nuclei were stained with DAPI. The scale bar (8 μm) is shown as a black box.

3.3. Identification of Functional Nuclear/Nucleolar Localization Sequences of Protein VII

To identify motifs involved in nuclear localization of protein VII (Figure 3A,D), plasmids expressing mutant protein VII (containing substitution of arginines with alanines in potential NLSs) fused to the HA tag [33] were constructed (Figure 3B,E). Vero cells were transfected with individual mutant plasmid DNAs and analyzed by indirect immunofluorescence assay at 48 h post transfection. As seen in Figure 3C, substitution of arginines with alanines in individual potential NLS1 (Panels g–i), NLS2 (j–l), NLS3 (Panels m–o) or NLS4 (Panels p–r) did not alter the nuclear localization of protein VII (Panels d-f). However, substitution of arginines with alanines (Figure 3F) in two (Panels g–i) or three (Panels j–l) potential NLS sites localizes protein VII both in the nucleus and the cytoplasm. Interestingly, substitution of arginines with alanines in four potential NLS sites abolishes the nuclear localization of protein VII (Panels m–o).

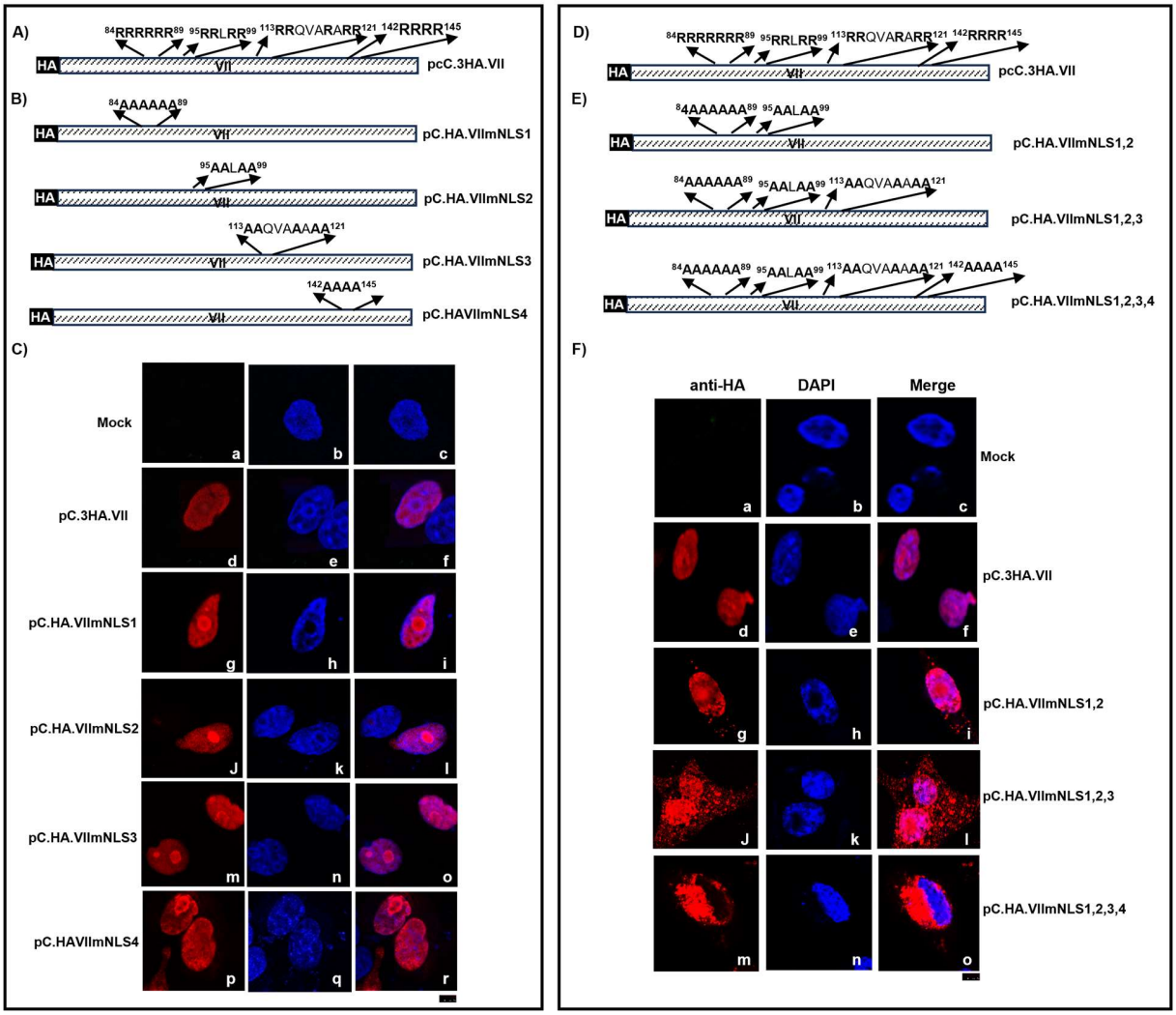

Figure 3. Analysis of nuclear localization signals (NLSs) of BAdV-3 protein VII. (**A**,**D**). Schematic representation of BAdV-3 protein VII in plasmids. The numbers depict the amino acid number. Potential

nuclear localizations signals (NLSs) are depicted. The name of the plasmid is on the right of the panel. Hemagglutinin Tag (HA). (**B**,**E**). Schematic representation of mutant protein VII. The numbers depict the amino acid number. Arginine to alanine mutation of potential nuclear localizations signals (NLSs) is depicted. The name of the plasmid is on the right of the panel. (**C**,**F**). Sub-cellular localization of protein VII. Vero cells transfected with indicated plasmid DNAs were fixed with 3.7% formaldehyde and 0.2% TritonX-100 at 48 h post transfection and visualized by indirect immunofluorescence using anti-HA MAb. The nuclei were stained with DAPI. The scale bar for panels C and F (5 μm) are shown as a black box.

The percentage of cells showing similar display of protein distribution is summarized in Supplementary File (Table S11).

To identify nucleolar localization sequences, Vero cells were transfected with individual mutant plasmid DNAs and analyzed by immunofluorescence assay at 48 h post transfection. As seen Figure 4, fluorescent signals for protein VII and nucleolin coincide with nucleolin in cells transfected with plasmid pC.HA.VII DNA, plasmid pC.HA.pVIImNLS1 DNA, plasmid pC.HA.VIIm NLS2, pC.HA.VIImNLS3 DNA, plasmid pC.HA.VIImNLS4 DNA, plasmid pC.HA.VIIm1,2 DNA and plasmid pC.HA.VIImNLS1,2,3 DNA. However, fluorescent signals for protein VII expressed in cells transfected with plasmid pC.HA.VIIm,1,2,3,4 DNA do not appear to coincide with nucleolin.

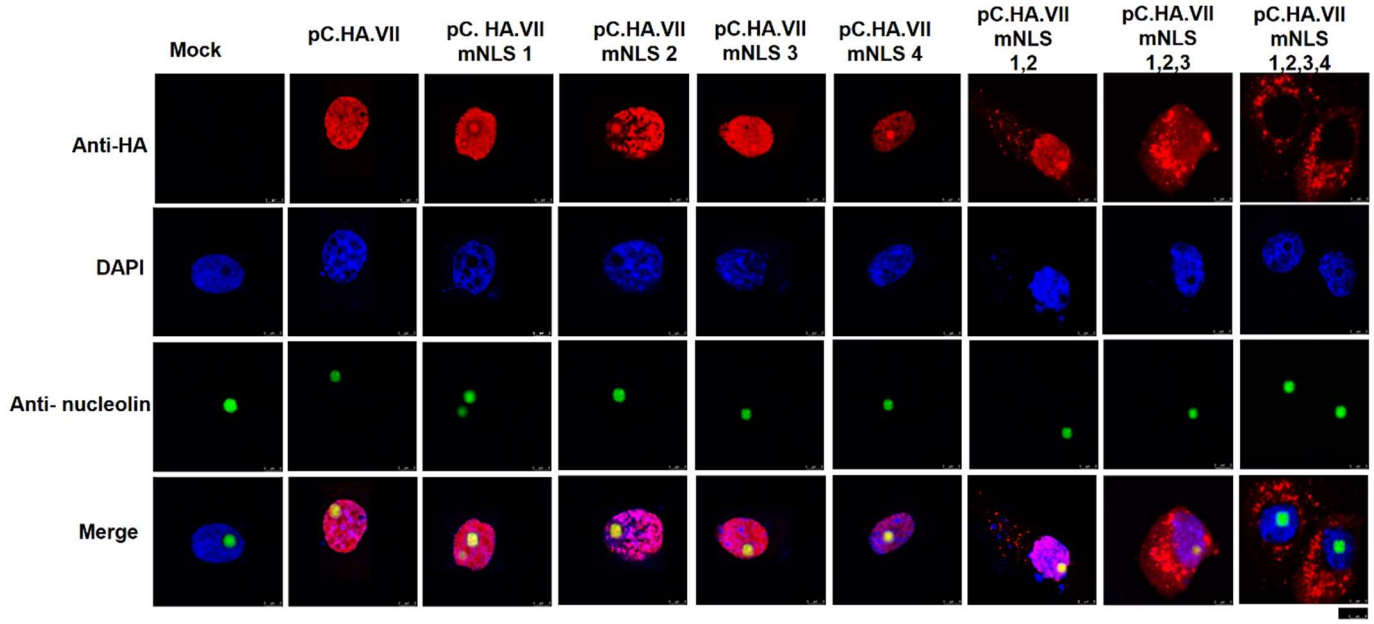

Figure 4. Analysis of nucleolar localization sequences (NoLSs) of BAdV-3 protein. Schematic representation of BAdV-3 protein VII is shown in Figure 3A,D. Vero cells transfected with indicated plasmid DNAs were fixed with 3.7% formaldehyde and 0.2% TritonX-100 at 48 h post transfection and visualized by indirect immunofluorescence using anti-HA MAb and anti nucleolin rabbit sera. The nuclei were stained with DAPI. The scale bar (8 μm) is shown as a black box.

The percentage of cells showing similar display of protein distribution is summarized in Supplementary File (Table S12).

3.4. Interaction of Protein VII with Importins/Transportin

To identify the import receptor(s) involved in the nuclear transportation of protein VII, purified individual GST-importin fusion protein or GST-transportin-3 fusion protein was incubated with lysates of cells transfected with plasmid pC.HA.VII DNA or plasmid pC.IVa2 DNA. Finally, the protein complexes were pulled down by GST beads and analyzed by Western blot using specific sera. As seen in Figure 5A, protein VII appears to interact with importins α1 (Lne 5), β1 (Lane 12) and transportin-3 (Lane 13) but not with α3

(Lane 6), α5 (Lane 7), α7 (Lane 8), α9 (Lane 9), α11 (Lane 10) or α13 (Lane 11). Similarly, no interaction could be detected between protein VII and GST (Lane 2). As expected, [5] IVa2 interacted with importin α1 (Figure 5B, Lane 3), but not with importin α3 (Figure 5A, Lane 3). Input protein VII (Figure 5A, Lane 4) and input protein IVa2 (Figure 5B [Lane 2]) are shown.

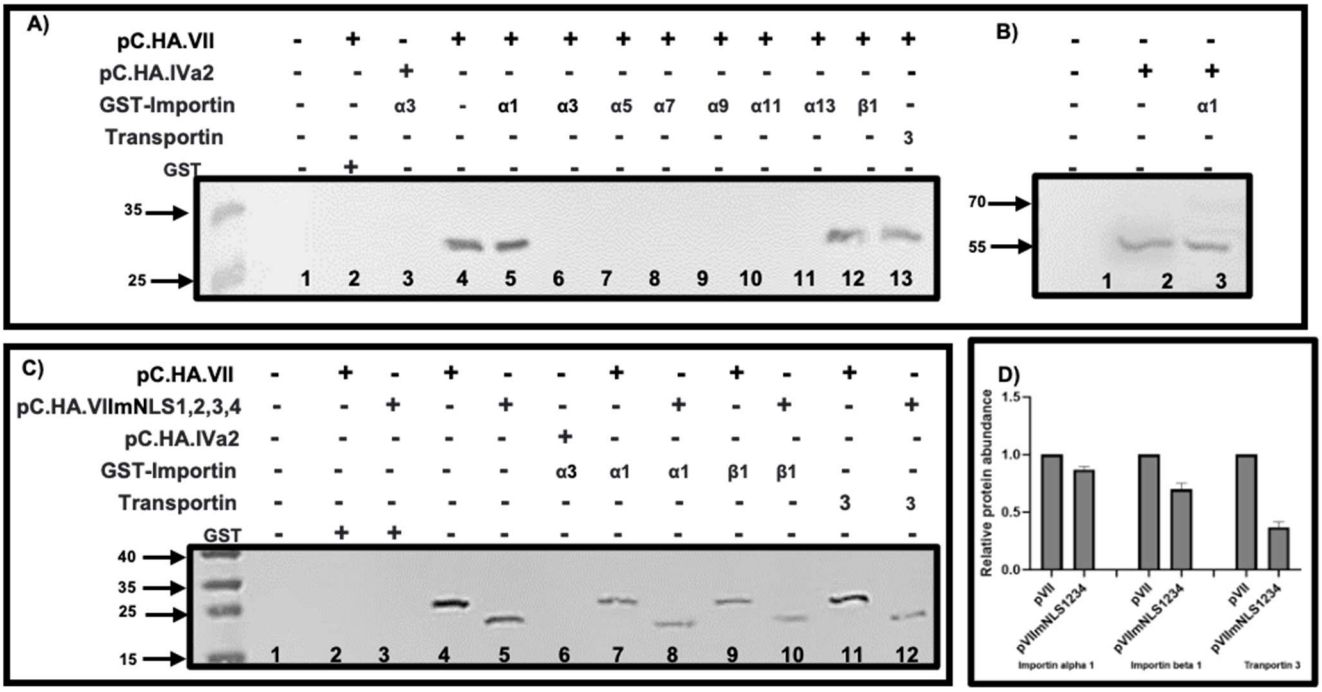

Figure 5. Interactions of protein VII with nuclear transport receptors. (**A**,**C**). Western blots. Purified GST-transport receptor fusion proteins were individually mixed with lysates of 293T cells transfected with indicated plasmids. The complexes were pulled down by centrifugation and visualized in Western blot using anti HA MAb. (**B**). Input HA.IVa2 and positive control [5] are shown. (**C**). Purified GST importin α1, β1 and transportin-3 proteins were individually mixed with lysates of 293T cells transfected with plasmid pC.HA.VII DNA or pC.HA.VIImNLS1,2,3,4 DNA. The complexes were pulled down by centrifugation and visualized in Western blot using anti HA MAb (**D**). The values of panel C (Lanes 7–12) were analyzed by GraphPad Prism, version 10 (GraphPad Software, Inc., La Jolla, CA, USA). The values represent the average from three independent experiments, and error bars represent standard deviations.

To identify whether NLS1−4 motifs are sufficient to bind importins/transportin-3, purified GST-importin fusion proteins or GST-transportin-3 fusion protein were incubated with lysates of cells transfected with plasmid pC.HA.VII DNA, plasmid pC.HA.VIImNLS 1,2,3,4 DNA or plasmid pC.HA.IVa2 DNA. Finally, the protein complexes were pulled down by GST beads and analyzed by Western blot using specific sera. As seen Figure 5C,D, importin α1 (Lane 8), importin β1 (Lane 10) and transportin-3 (Lane 12) interacted less efficiently with protein VIIm1,2,3,4 than protein VII (importin α1 [Lane 7]; importin β1 [Lane 9]; or transportin-3 [Lane 11]). Input protein VII (Figure 5C [Lane 4]) and VIImNLS1,2,3,4 (Figure 5C [Lane 5]) are shown.

3.5. Construction of BAdV-3 with Strep-Tagged Protein VII

To study the interactions between *BAdV-3* protein VII and other viral and cellular proteins during viral infection, we constructed recombinant BAV.VII.ST. Initially, we constructed a plasmid pC.HA.VII.Strep containing Strep-Tag II motif inserted in protein VII (Figure 6A) and analyzed the expression of recombinant protein in transfected cells. As seen in Figure 6B, Western blot analysis identified a protein of 26 kDa in 293T cells transfected with plasmid pC.HA.VII.Strep DNA or plasmid pC.HA.VII DNA (Figure 6B). Similarly,

immunofluorescence analysis demonstrated nuclear location of protein VII in Vero cells transfected with plasmid pC.HA.VII.Strep DNA or plasmid pC.HA.VII DNA (Figure 6C). However, compared to protein VII, there appeared to be some difference in the distribution of protein VII-Strep-tag II in the nucleus (Figure 6C).

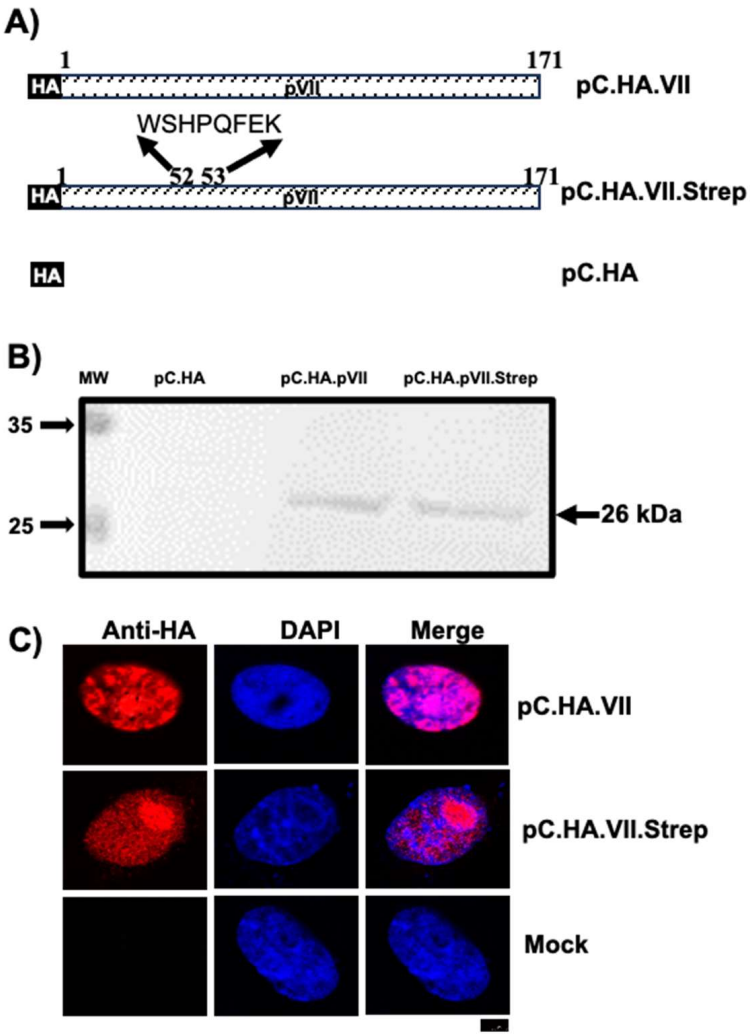

Figure 6. Analysis of protein HA.VII.Strep. (**A**). Schematic representation of proteins expressed by plasmids. The amino acid numbers are depicted. The Strep Tag II sequence is depicted. Hemagglutinin Tag (HA). (**B**). Western blot. Proteins from lysates of plasmid DNA transfected cells were separated by 12% SDS-PAGE, transferred to nitrocellulose and visualized by Western blot using anti-HA MAb. Molecular weight markers (MW). (**C**). Vero cells transfected with indicated plasmid DNAs were fixed with 3.7% formaldehyde and 0.2% TritonX-100 and analyzed by indirect immunofluorescence using anti-HA MAb. The scale bar (2.5 μm) is shown as a black box.

Since insertion of Strep-Tag II did not alter the expression or subcellular localization of protein VII, we constructed a recombinant plasmid pUC304a.VII.Strep containing full-length genomic DNA of BAV304a with modified protein VII (protein VII containing insertion of the Strep Tag (Figure 7A). VIDO DT1 cells transfected with plasmid pUC304a DNA (Figure 7A) produced cytopathic effects in 7 days (Figure 7B, Panels a–c). Similarly, transfection of VIDO DT1 cells with plasmid pUC304a.VII.Strep DNA (Figure 7A) produced cytopathic effect in 7 days (Figure 7B, Panels g–i). The infected cells were harvested 15 days post transfection, freeze-thawed three times, and recombinant virus designated BAV.VII.ST was isolated and propagated in MDBK cells. The recombinant BAV.VII.ST was analyzed by DNA sequencing.

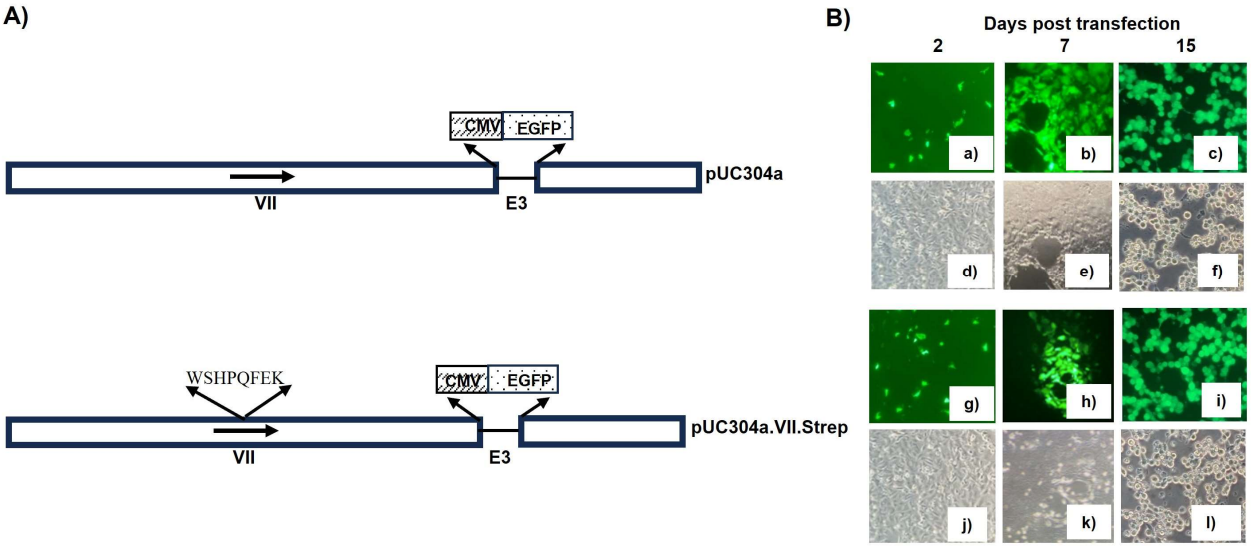

Figure 7. Isolation of recombinant BAV.VII.ST (**A**). Schematic representation of BAdV-3 genomic DNA. The name of the plasmids is depicted on right side of the panel. The sequence of Strep Tag II (WSHPQFEK) is depicted. The arrows in the genome sequence determine the direction of transcription. Human cytomegalovirus immediate early promoter (CMV); enhanced green fluorescent protein (EYFP). (**B**). Fluorescent microscopy. VIDO DT1 cells transfected with indicated plasmid DNA were observed for the appearance of green fluorescent cells and cytopathic effects. The numbers represent the days after transfection. Phase contrast (Panels d–f and j–l).

3.6. Characterization of BAV.VII.ST

To determine whether the insertion of the Strep Tag in BAdV-3 protein VII affects the viral protein expression in infected cells, virus-infected MDBK cells were analyzed by immunofluorescence assay and Western blot using protein-specific sera. As seen in Figure 8A, immunofluorescence assay demonstrated no detectable difference in the subcellular localization of protein VII in BAV304a- or BAV.VII.ST-infected cells. Similarly, Western blot analysis (Figure 8B) showed no detectable difference in the expression of protein VII in BAV304a- or BAV.VII.ST-infected cells. Moreover, the expressions of other viral proteins including DBP (early) and IVa2 (intermediate) or VIII (late) appeared similar in BAV304a- or BAV.VII.ST-infected cells.

To determine the effect of Strep Tag insertion on BAV.VII.ST replication, we performed a single cycle growth assay. Briefly, MDBK cells were infected with a MOI of five. At indicated times post infection, infected cells were collected, freeze-thawed 3–5 times and the virus titer was determined by FFU/mL. As seen in Figure 8C, BAV304a and BAV.VII.ST demonstrated similar growth characteristics.

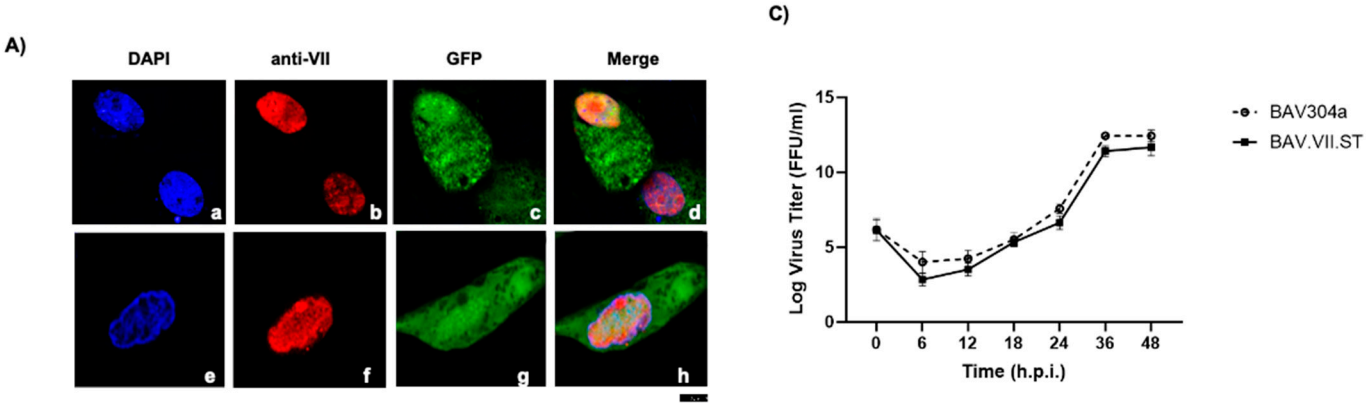

Figure 8. *Cont.*

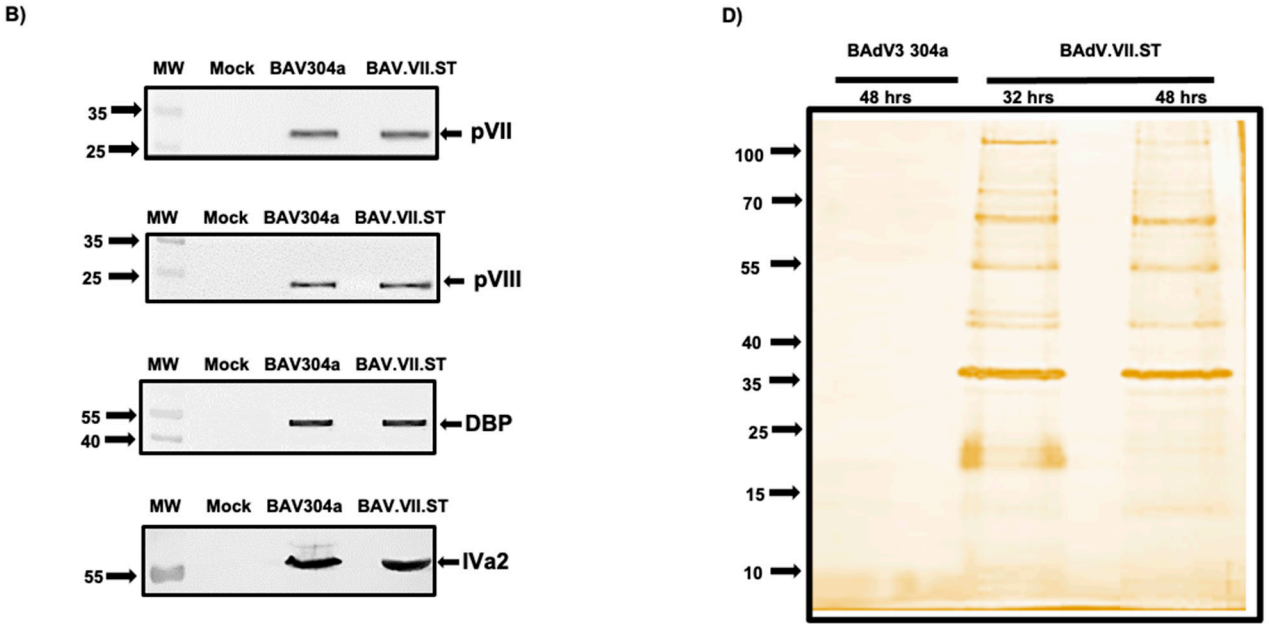

Figure 8. Analysis of BAV.VII.ST. (**A**). Sub-cellular localization of protein VII. MDBK cells were infected with indicated virus. After 48 h post infection, the cells were fixed with 3.7% formaldehyde and 0.2% TritonX-100, and analyzed by direct fluorescence (Panels c,g) or indirect fluorescence using anti-VII sera (Panels a,b,d; e,f,h) under a fluorescent microscope. The scale bar (5 μm) is shown as a black box (**B**). Western blot. Proteins from lysates of indicated virus infected cells were separated by 12% SDS-PAGE a, transferred to nitrocellulose and probe in Western blot using protein specific-sera. The name of the protein is depicted on the right of the panel. (**C**). Virus titer. Monolayers of MDBK cells were infected with indicated viruses. At different times post infection, the infected cells were collected, freeze-thawed and titrated on MDBK cells. Values represent average of two independent repeats and error bars represent S.D. (**D**). Silver staining. Proteins purified from BAdV304a- or BAV.VII.Strep-infected MDBK cells by streptactin Sepharose beads at indicated times post infection were separated by10% SDS-PAGE. The gel was stained with silver stain. Position of the molecular weight markers is shown on the left of the panel.

3.7. Purification and Identification of Cellular/Viral Proteins Interacting with Protein VII

Since Strep Tag introduction did not influence viral replication and protein VII functions, BAV.VII.ST was used to determine the viral/cellular proteins interacting with protein VII. Briefly, MDBK cells were infected with BAV404a or BAV.VII.ST at MOI of five. At 32 and 48 h post infection, proteins from the lysates of infected cells were purified using Strep-tactin Sepharose beads. Proteins in the purified samples were separated by 10% SDS-PAGE followed by silver staining. As shown in Figure 8D, protein bands were detected by the silver staining of samples purified from BAV.VII.ST post-infected MDBK cells while no band was observed in protein samples purified from BAV304a-infected MDBK cells. Once Strep-Tagged protein complexes were purified and concentrated, they were sent for LC-MS/MS analysis to the University of Victoria-Genome BC proteomics Centre. A number of viral or cellular proteins were identified from the protein complexes extracted 32 and 48 h post infection. In fact, four viral (Table 1) and several cellular proteins (Supplementary File S2) including other cellular proteins (Table S2), ribosomal proteins (Table S3), mitochondrial proteins (Table S4), cytoskeleton proteins (Table S5), nuclear proteins (Table S6) and nucleolar proteins (Table S7) were observed. We filtered the list of proteins in two independent ways: protein probabilities and number of peptides. In detail, we assigned filter criteria as 100% probability in one of the two samples and more than two peptides. Each protein had to be above both filter criteria to be displayed.

Table 1. Viral proteins identified from LC-MS/MS analysis.

Protein	Accession #	MW	Protein Probability (32 h)	Protein Probability (48 h)	# of Peptides
IVa2	P03273 [7]	51 kDa	86%	100%	2
pVIII	Q03556	15 kDa	100%	100%	4
Hexon	P03278 [3]	103 kDa	100%	100%	5
Fiber	Q03553	102 kDa	100%	100%	5

3.8. Interaction between Proteins VII-IVa2 and Proteins VII-VIII

Since proteins VIII and IVa2 are involved in stabilization of capsid [34] and genome assembly [5], respectively, initially, we analyzed the viral protein interaction by biomolecular-fluorescence complementation (BiFC) assay [34]. Yeast competent cells S288c co-transformed with plasmid (pGC.pVII + pGN.IVa2, pGC.pVII + pGN.pVIII, pGC.pVII + pGN or pGN.IVa2 + pGC.pV) DNAs (Figure 9A) were plated out in a dropout medium devoid of histidine and uracil and analyzed by confocal microscopy. As expected, green fluorescence was observed in yeast cells co-transformed with plasmid pGN.IVa2 + pGC.pV DNAs (Figure 9B). Similarly, green fluorescence could be observed in yeast cells co-transformed with plasmid pGC.pVII + pGN.IVa2 DNAs or plasmid pGC.pVII + pGN.pVIII DNAs (Figure 9B). No such green fluorescence could be observed in yeast cells co-transformed with plasmids pGC.pVII + pGN DNAs or plasmids pGC + pGN DNAs (Figure 9B).

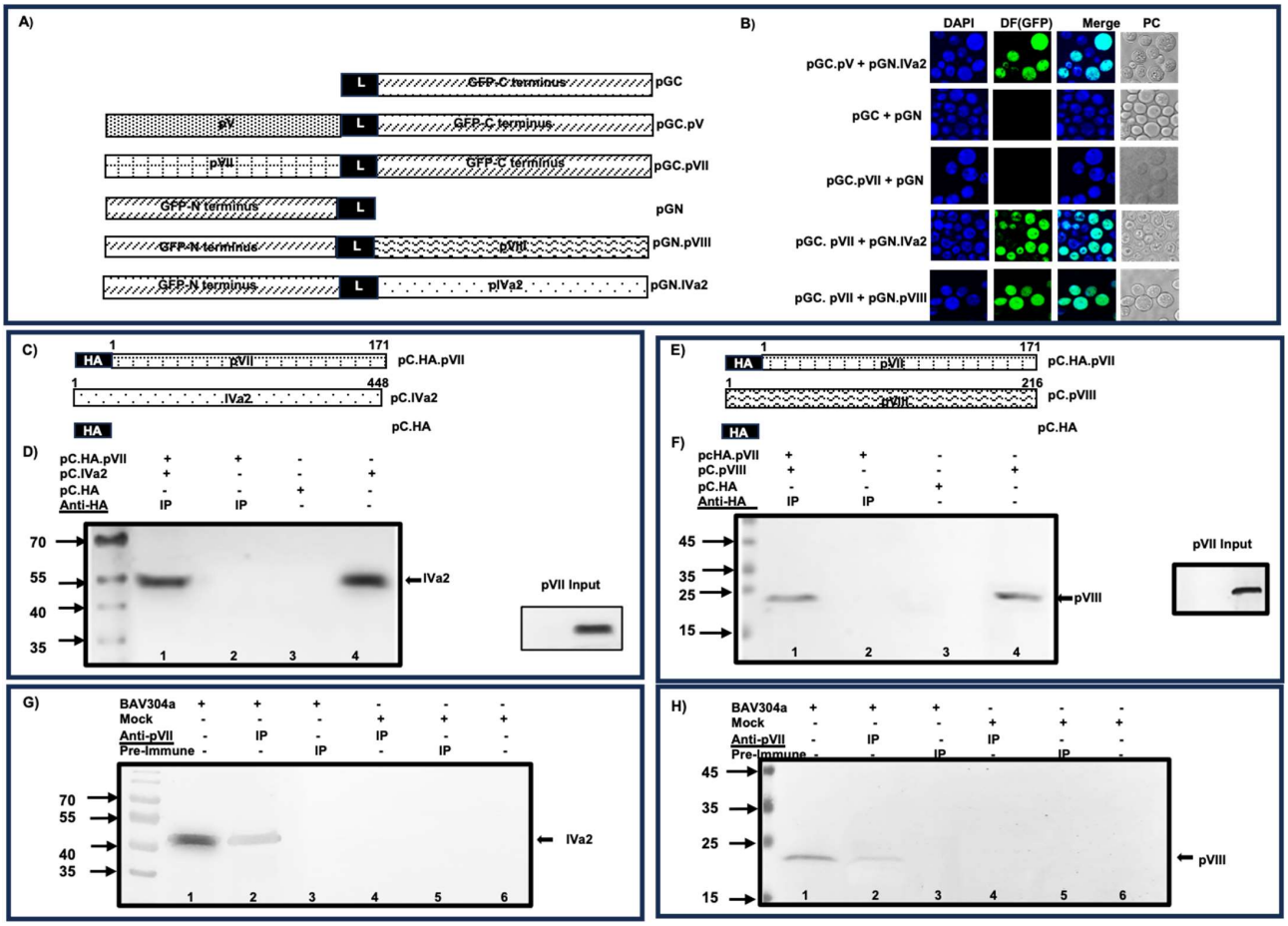

Figure 9. Interaction of BAdV-3 protein VII with other viral proteins. (**A**,**C**,**E**). Schematic representation of proteins expressed by plasmids. The name of the plasmid is depicted on the right side of the panel. Hemagglutinin Tag (HA). Linker region (L). Green fluorescent protein N-terminus (GFP-N). Green florescent

protein-C terminus (GFP-C). (**B**). Biomolecular fluorescence complementation assay (BiFC). Yeast S288c cells co-transformed with indicated plasmid DNAs were incubated on selective media and observed under confocal microscope. Direct fluorescence (DF). Phase contrast (PC). (**D**,**F**). Transfected cells. Proteins from lysates of cells co-transfected with indicated plasmids were immunoprecipitated with anti-HA Mab. The immunoprecipitated complexes or lysates of cells transfected with indicated plasmids were separated by 12% SDS-PAGE, transferred to nitrocellulose and probed in Western blot using anti-IVa2 sera (**D**) and anti-VIII sera (**F**). (**G**,**H**). BAdV-3 infected cells. Proteins from lysates of mock- or BAdV-3-infected cells immunoprecipitated with anti-VII sera were separated by 12% SDS-PAGE, transferred to nitrocellulose and probed in Western blot with anti-IVa2 (**G**) and anti-VIII sera (**H**).

To further confirm interactions between proteins VII and IVa2, 293T cells were co-transfected with indicated plasmids (Figure 9C). After 48 h post transfection, proteins from the lysates of co-transfected cells were immunoprecipitated (Figure 9D) using anti-HA MAb and analyzed by Western blot using anti-IVa2 sera [5]. As seen in Figure 9D, a IVa2-specific protein band could be detected in cells co-transfected with plasmid pC.HA.pVII + pC.IVa2 DNAs (Lane 1). A similar protein could be detected in cells transfected with individual plasmid pC.IVa2 DNA (Lane 4) in Western blot using anti-IVa2 sera. No such protein could be detected in cells co-transfected with plasmid pC.IVa2 + pC.HA DNAs and immunoprecipitated with anti-HA MAb (Lane 2) or transfected with individual plasmid pC.HA DNA in Western blot using anti-IVa2 sera (Lane 3).

Similarly, interactions between protein VII and protein VIII were confirmed by co-immunoprecipitation/Western blot assays. 293T cells were co-transfected with indicated plasmid DNAs (Figure 9 E). After 48 h post transfection, proteins from the lysates of co-transfected cells were immunoprecipitated (Figure 9 F) using anti-HA MAb and analyzed by Western blot using anti-pVIII sera [23]. As seen in Figure 9 F, protein VIII-specific protein could be detected in cells co-transfected with plasmid pC.HA.pVII + pC.pVIII DNAs (Lane 1). A similar protein could be detected in cells transfected with individual plasmid pC.VIII DNA in Western blot using anti-VIII sera (Lane 4). No such protein could be detected in the cells co-transfected with plasmid pC.pVIII + pC.HA DNAs and immunoprecipitated with anti-HA (Lane 2) or transfected with individual plasmid pC.HA (Lane 3) in Western blot using anti-pVIII sera.

Finally, the interactions of protein VII with protein IVa2 and protein VIII were verified in infected cells. MDBK cells were infected with BAV304a. After 48 h post infection, the proteins from the cell lysates were immunoprecipitated with the indicated sera and co-immunoprecipitated proteins were detected in Western blots using viral protein-specific sera. As seen in Figure 9G, IVa2-specific protein could be detected in infected cells immunoprecipitated with anti-pVII sera (Lane 2). A similar protein could be detected in BAV304a-infected cells in Western blot using anti-IVa2 sera (Lane 1). No such protein could be detected in mock-infected cells immunoprecipitated with anti-pVII sera (Lane 4), prebleed sera (Lane 5) or BAdV-3-infected cells immunoprecipitated with preimmune sera (Lane 3)

Similarly, protein VIII-specific protein could be detected in BAdV-3-infected cells immunoprecipitated with anti-pVII sera (Figure 9H, Lane 2). No such protein could be detected in mock-infected cells immunoprecipitated by anti-pVII sera (Figure 9H, Lane 4) or pre-bleed sera (Figure 9H, Lane 5). As expected, Western blot analysis of proteins from BAV304a-infected cells detected IVa2 and protein VIII proteins using anti-IVa2 sera (Figure 9G, Lane 1) and anti-pVIII sera (Figure 9H, Lane 1), respectively.

3.9. Identification of Protein VII Domain Interacting with IVa2

To determine the domain of protein VII interacting with IVa2, we conducted the BiFC assay using plasmids expressing protein VII deletions/truncations (Figure 10A). Initially, random deletions spanning about 40 amino acid of protein VII were constructed. Results are summarized in Figure 10B. As expected, green fluorescence could be detected in yeast cells co-transfected with plasmid pGC.pVII + pGN.IVa2 DNAs. Similar green fluorescence

could be observed in yeast cells co-transformed with plasmids pGC.pVIId1 + pGN.IVa2 DNAs, plasmids pGC.pVIId2 + pGN.IVa2 DNAs or plasmids pGC.pVIId4 + pGN.IVa2 DNAs. No such fluorescence could be observed in yeast cells co-transformed with plasmids pGC.pVIId3 + pGN.IVa2 DNAs or plasmids pGC.pVII + pGN DNAs.

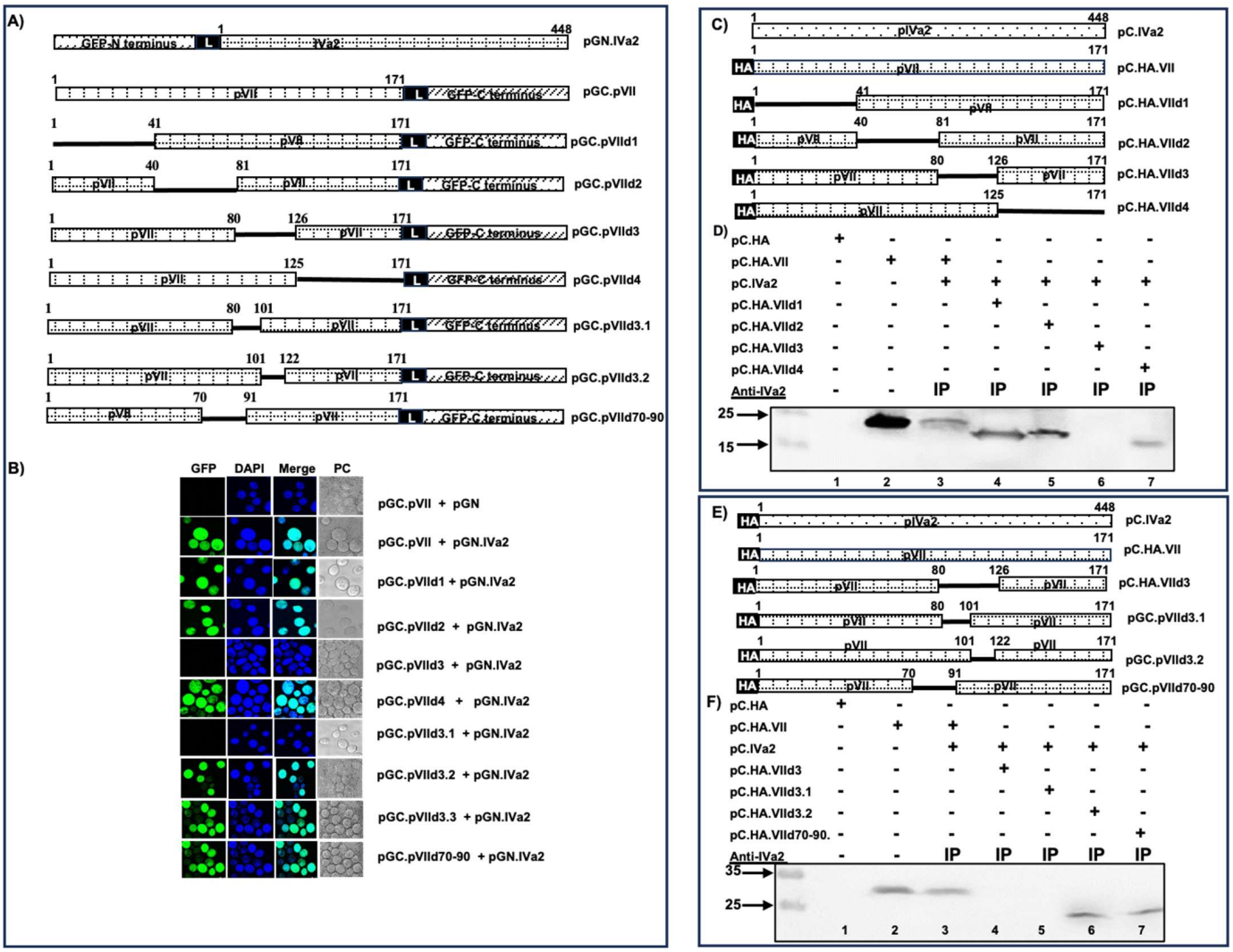

Figure 10. Identification of BAdV-3 protein VII domain(s) interacting with IVa2. (**A**,**C**,**E**). Schematic representation of plasmid DNAs. The name of the plasmid is depicted on the right side of the panel. Amino acid numbers are depicted. Solid black line represents deleted region. Hemagglutinin Tag (HA). Linker region (L). Green fluorescent protein N-terminus (GFP-N). Green florescent protein-C terminus (GFP-C). (**B**). Biomolecular fluorescence complementation assay (BiFC). Yeast S288c cells co-transformed with indicated plasmid DNAs were incubated on selective media and observed under confocal microscope. Direct fluorescence (DF). Phase contrast (PC). (**D**,**F**). Western blots. Proteins from the lysates of cells co-transfected with indicated plasmids were immunoprecipitated with anti-IVa2. The immunoprecipitated complexes or lysates of cells transfected with indicated plasmids were separated by 12% SDS-PAGE, transferred to nitrocellulose and probed in Western blot using anti-HA MAb.

Since no interaction was observed between IVa2 and protein VII (containing deletion of amino acids 81–125; pGC.pVIIId3), plasmids expressing mutant protein VII containing smaller deletions in amino acids 81–125 were constructed (Figure 10A). Green fluorescence could be observed in yeast cells co-transformed with plasmids pGC.VIId3.2 +pGN.IVa2 DNAs, plasmids pGC.VIId3.3 + pCN.IVa2 DNAs or plasmids pGC.VIId70−90 DNAs

(Figure 10B). No such fluorescence could be observed in yeast cells co-transformed with plasmids pGC.VIId3.1 + pGN.IVa2 DNAs (Figure 10B).

The BiFC analysis results were confirmed by co-immunoprecipitation assays using plasmids expressing HA-tagged protein VII deletions/truncation (Figure 10 C,E). Proteins from the lysates of 293T cells co-transfected with indicated plasmid DNAs were immunoprecipitated using anti-IVa2 sera and co-immunoprecipitated protein VII or protein from individual plasmid DNA-transfected cells was detected in Western blotting using and anti-HA MAb. As seen in (Figure 10D), an VII-specific protein could be detected in the cells co-transfected with plasmids pC.HA.VII + pC.IVa2 DNAs (Lane 3), plasmids pC.HA.VIId1 + pC.IVa2 DNAs (Lane 4), plasmids pC.HA.VIId2 + pC.IVa2 DNAs (Lane 5) and plasmids pC.HA.VIId4 + pC.IVa2 DNAs (Lane 7). No such protein could be observed in cells co-transfected with plasmids pC.HA.VIId3 + pC.IVA2 (Lane 6). Protein VII could be detected in cells transfected with plasmid pC.HA.VII DNA (Lane 2) but not in cells transfected with plasmid pC.HA DNA (Lane 1) in Western blotting using anti-HA Mab.

Similarly (Figure 10F), protein VII-specific protein could be observed in cells co-transfected with plasmids pC.HA.VII + pC.IVa2 DNAs (Lane 3), plasmids pC.HA.VIId3.2 + pC.IVa2 DNAs (Lane 6) or plasmids pC.HA.VIId70−90 + pC.IVa2 (Lane 7). No such protein could be detected in cells co-transfected with plasmids pC.HA.VIId3 + pC.IVa2 DNAs (Lane 4) or plasmids pC.HA.VIId3.1 +pC.IVa2 DNAs (Lane 5). Protein VII could be detected in cells transfected with plasmid pCHA.VII DNA (Lane 2) but not in cells transfected with plasmid pC.HA DNA (Lane 1) in Western blotting using anti-HA Mab. The input blots are shown in Supplementary File (Figure S1).

The results are summarized in Supplementary File (Table S8).

3.10. Identification of Protein VII Domain Interacting with Protein VIII

To identify the domain of protein VII interacting with protein VIII, we performed BiFC assay using plasmids expressing protein VII deletions/truncations (Figure 11A). Results are summarized in Figure 11B. Green fluorescence was observed in yeast cells co-transformed with plasmids pGC.pVII + pGN.pVIII DNAs, plasmids pGC.pVIId1 + pGN.pVIII DNAs, plasmids pGC.pVIId2 + pGN.pVIII DNAs and plasmids pGC.pVIId3 + pGN.pVIII DNAs. No such green fluorescence could be observed in yeast cells co-transfected with plasmids pGC.VIId4 + pGN.VIII.

Since no interaction was observed between protein VII and protein VIII (containing deletion of amino acids 125–171), plasmids expressing mutant protein VII containing smaller deletions in amino acids 125–171 were constructed (Figure 11A). The results are summarized in Figure 11B. Green florescence could be observed in yeast cells co-transfected with plasmids pGC.VIId4.1 + pGN.pVIII DNAs, plasmids pGC.VIId4.2 + pGN.pVIII DNAs and plasmids pGC.VIId4.3 + pGN.pVIII DNAs. No such florescence could be observed in yeast cells co-transfected with plasmids pGC.pVIId126−137 + pGN.pVIII DNAs.

The BiFC analysis results were confirmed by co-immunoprecipitation assays using plasmids expressing HA-tagged protein VII deletions/truncation (Figure 12A,C,E). Proteins from the lysates of 293T cells co-transfected with indicated plasmid DNAs were immunoprecipitated using anti-VIII sera, and co-immunoprecipitated protein VII protein or protein from individual plasmid DNA transfected cells was detected in Western blot using and anti-HA MAb. As seen in (Figure 12B), protein VII-specific protein could be detect in the cells transfected with plasmid pC.HA.VII DNA (Lane 2) or co-transfected with plasmids pC.HA.VII + pC.VIII DNAs (Lane 3), plasmids pC.HA.VIId1 + pC.VIII DNAs (Lane 4), plasmids pC.HA.VIId2 + pC.VIII DNAs (Lane 5) and plasmids pC.HA.VIId3 + pC.VIII DNAs (Lane 6). No such protein could be observed in cells transfected with plasmid pC.HA DNA (Lane 1) or co-transfected with plasmids pC.HA.VIId4 + pC.VIII DNAs (Lane 7).

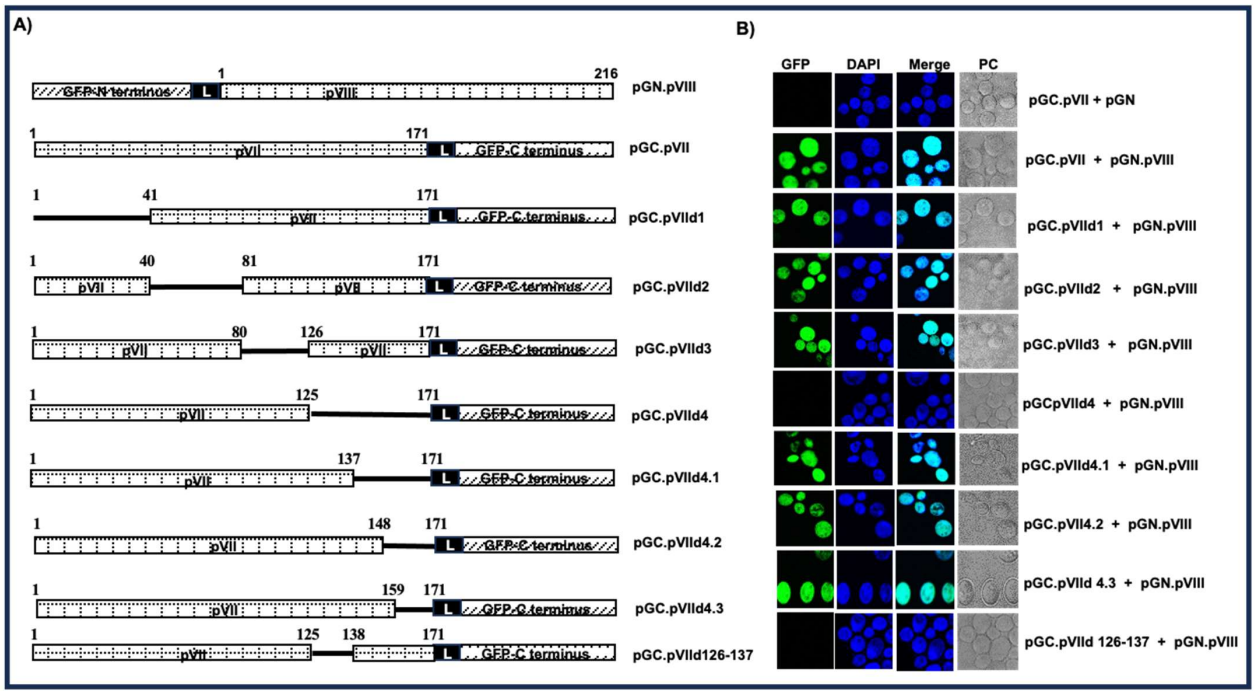

Figure 11. Identification of BAdV-3 protein VII domain(s) interacting with protein VIII by BiFC. (**A**). Schematic representation of proteins encoded by plasmid DNAs. The name of the plasmid is depicted on the right side of the panel. Amino acid numbers are depicted. Solid black line represents deleted region. Linker region (L). Green fluorescent protein N-terminus (GFP-N). Green florescent protein-C terminus (GFP-C). (**B**). Biomolecular fluorescence complementation assay (BiFC). Yeast S288c cells co-transformed with indicated plasmid DNAs were incubated on selective media and observed under confocal microscope. Direct fluorescence (DF). Phase contrast (PC).

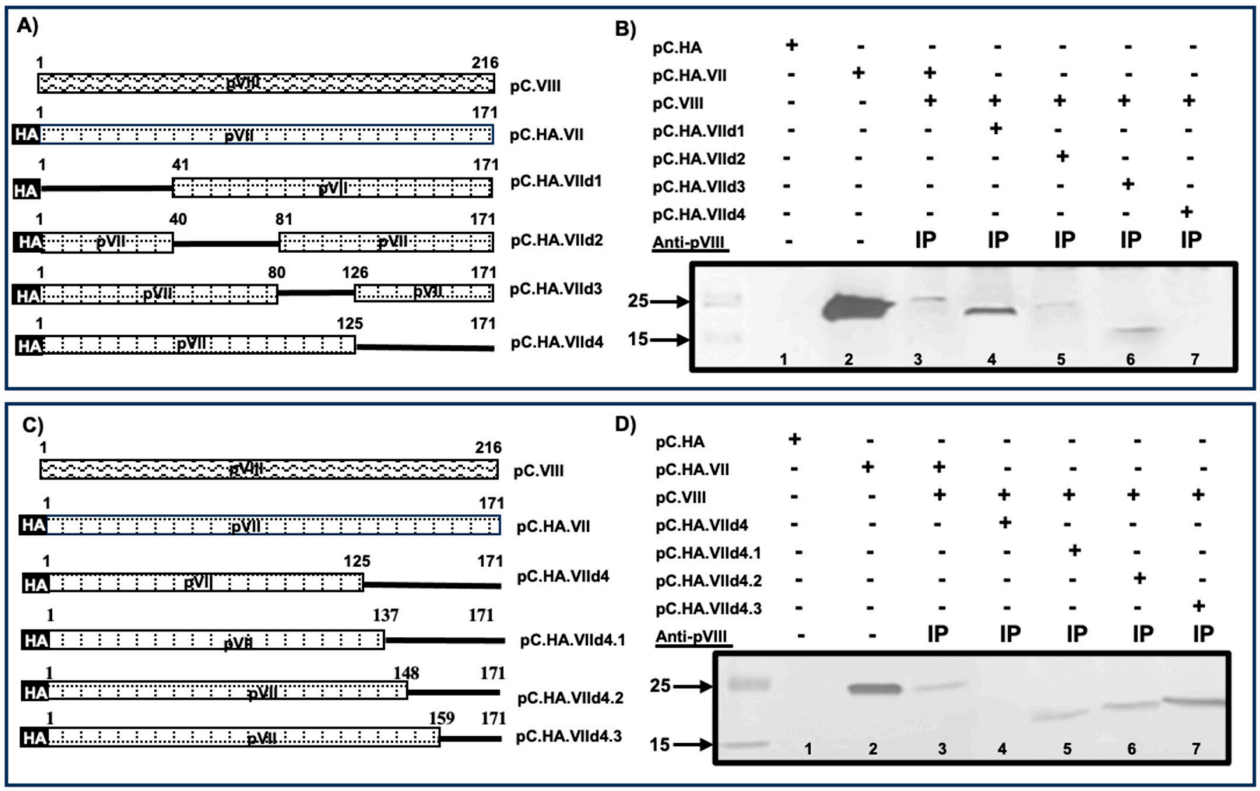

Figure 12. *Cont.*

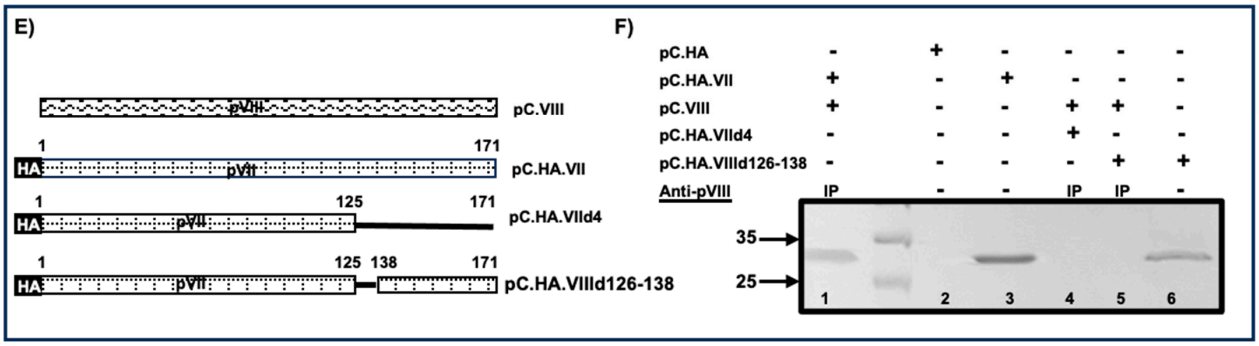

Figure 12. Identification of BAdV-3 protein VII domain(s) interacting with protein VIII by Western blot. (**A**,**C**,**E**) Schematic representation of proteins expressed by plasmid DNAs. The name of the plasmid is depicted on the right side of the panel. Amino acid numbers are depicted. Solid black line represents deleted region. Hemagglutinin Tag (HA). (**B**,**D**,**F**). Proteins from the lysates of cells co-transfected with indicated plasmid DNAs were immunoprecipitated with anti-pVIII. The immunoprecipitated complexes or lysates of cells transfected with indicated plasmids were separated by 12% SDS-PAGE, transferred to nitrocellulose and probed in Western blot using anti-HA MAb. Immunoprecipitation (IP). Molecular weight markers are shown on the left of the panel.

Similarly (Figure 12D), protein VII-specific protein could be observed in cells co-transfected with plasmids pC.HA.VII + pC.VIII DNAs (Lane 3), plasmids pC.HA.VII4.d1 + pC.IVa2 DNAs (Lane 5) or plasmids pC.HA.VIId4.2 + pC.VIII (Lane 6) DNAs (Lane 7) or plasmids pC.HA.VIId3 + pC.VIII DNAs (Lane 7). No such protein could be detected in cells co-transfected with plasmids pC.HA.VIId4 + pC.VIII DNAs (Lane 4).

Finally (Figure 12F), protein VII-specific protein could be observed in cells co-transfected with plasmids pC.HA.VII + pC.VIII DNA (Lane 1) or transfected with plasmid pC.HA.VII DNA (Lane 3). No such protein could be detected in cells co-transfected with plasmids pC.HA.VIId4 + pC.VIII (Lane 4) or plasmids pC.HA.VIId126-137 (Lane 5). The input blots are shown in Supplementary File (Figure S2).

4. Discussion

Protein–protein interactions (PPIs) play a critical role in different steps of viral replication. Like with other viruses, production of an infectious adenovirus involves interaction of viral proteins with host proteins [35–39] and other viral proteins [5,40–42]. Understanding these PPIs are important to predict the sub-cellular localization and functions of the adenoviral proteins.

Protein VII is a multifunctional protein [11] which appears to be involved in many stages of the viral life cycle including endosomal escape of incoming infectious virus [14], transcription of early viral genes [12,13,43], internalizing the viral genome into nuclei [7], protecting viral DNA from cellular DNA damage response [44] and maturation of the virus particle [45,46]. The multiple functions performed by protein VII could be inherent or acquired by interacting with other cellular/viral proteins. Although structural analysis of adenovirus has provided valuable information about interactions of major and minor capsid proteins, little structural information is available regarding the interaction of virion core proteins including protein VII with other viral proteins [40,42,47]. Biochemical analysis suggested that human adenovirus protein VII interacts with protein IIIa [48], 52K [48], protein IVa2 [49] and protein V [41]. Since earlier studies have demonstrated differences in the structure and function [50–53] of colinear proteins [15] encoded by members of *Mastadenovirus* genus, we characterized the functional domains of BAdV-3 protein VII.

Protein VII appears to be actively transported to the nucleus/nucleolus of the cell as GFP-β-gal (cytoplasmic protein) fused to protein VII is predominantly localized to the nucleus of the transfected cell. Active nuclear transport of protein utilizes single or multiple NLSs (classical or non-classical) [54,55]. Similarly, analysis of nuclear transport

of adenoviral proteins has suggested the use of single [4,56] or multiple NLSs [3,57]. Like HAdV-5 [7], BAdV-3 protein VII also appears to use multiple NLSs. However, in contrast to HAdV-5 [7], the mutation (all arginine to alanine) of four NLSs could abolish the nuclear localization of protein VII. Since four NLSs are localized in non-conserved C-terminus of BAdV-3 protein VII, it is possible that localization of mutant protein VII predominantly in the cytoplasm (unlike HAdV-5 [7]) could be due to the difference in amino acid sequences of protein VII encoded by BAdV-3 and HAdV-5. Similar observations have been reported for the BAdV-3 100K protein [17].

Active nuclear transportation of adenoviral proteins uses single [5,17,23,58] or multiple [4,7,59] receptor-mediated pathways. Like HAdV-5 [7], BAdV-3 protein VII appears to utilize multiple receptors (importin-α1, importin-β1 and transportin-3) for nuclear transport. Moreover, the use of multiple NLSs and alternative nuclear receptor pathways may create a redundancy, which increases the efficiency of nuclear transport (to perform important functions) and prevents the nuclear import receptors from becoming a rate-limiting factor during protein VII nuclear localization.

Nucleolar transport of viral proteins involves interaction of viral sequences rich in basic residues (arginines and lysines) with nucleolar resident protein or RNA [60]. In addition, viral proteins utilize overlapping [61], non-overlapping [62] or both [3] (overlapping and non-overlapping NLSs/NoLSs) for transport to both the nucleus and nucleolus. Earlier, we demonstrated that while BAdV-3 IVa2 localizes to the nucleolus using non-overlapping NoLS/NLS [5], BAdV-3 protein V localizes to the nucleolus using both overlapping and non-overlapping NoLS/NLS [3]. The mutation (all arginine to alanine) of single, double or triple NLSs could not abolish the nucleolar localization of protein VII. However, mutation of (all arginine to alanine) four NLSs could abolish the nucleolar localization of the protein, suggesting that BAdV-3 protein VII contains overlapping NoLS/NLS.

An earlier report suggested that adenovirus protein VII interacts with IVa2 [49]. Our demonstration of interaction between BAdV-3 protein VII and IVa2 confirms earlier observations. Since IVa2 appears essential for both genome packaging and assembly [63], it was speculated that interaction between pVII and IVa2 may be required for packaging of DNA complexed with protein VII [49]. However, a recent report suggested the production of virus particles in the absence of protein VII, leading to the conclusion that protein VII is not required for genome encapsidation and virus assembly [14].

The adenovirus genome is tightly associated with about 800 copies of protein VII [64]. Earlier, we [5] and others [2] have demonstrated that adenovirus protein V interacts with IVa2 [5] and protein VIII [2]. Here, we demonstrate that protein VII interacts with IVa2 and protein VIII. Since protein V acts as a bridge between adenovirus core and capsid by binding to penton base and protein VI [37,65], it is possible that the interaction of protein VII with protein VIII and IVa2 further helps in connecting the core of the virus with the inner surface of the capsid [66], thus maintaining the integrity of the viral capsid. Interestingly, human adenovirus-5 virions devoid of protein VII [67] or expressing a mutant protein VIII [34,68] appear to be less thermostable than wild-type human adenovirus-5.

The N-terminus including adenovirus protease cleavage site appears to be highly conserved among protein VII encoded by other *Mastadenoviruses* [1]. The conserved protease cleavage site appears to be utilized in different members of *Mastadenovirus* genus. In fact, recent Cryo-EM studies has revealed the presence of only cleaved N-terminus protein VII (amino acid 14–24; VIIn2) in the hexon cavities [40]. Interestingly, analysis of protein VII deletions/truncations, identified amino acids 91–101 and amino acids 126–137 of protein VII as the regions interacting with IVa2 and protein VIII, respectively, which is part of mature protein VII. Few amino acids 92, 93, 95 of the 91–101 region and amino acids 127, 129, 130, 135 of region 126–137 appear conserved among protein VII encoded by members of *Mastadenovirus* genus. Since IVa2 and protein VIII appear to interact with non-conserved regions of protein VII, it would be interesting to determine whether the functions associated with these interactions are conserved among the members of *Mastadenovirus* genus.

In conclusion, here, we report that BAdV-3 protein VII localizes to nucleus/nucleolus using redundant nuclear/nucleolar localization signals/sequences and multiple nuclear transport receptors. Unlike HAdV-5 (7), BAdV-3 protein VII containing the deletion of potential nuclear localization signals localizes to the cytoplasm of transfected cells. Moreover, we demonstrate that non-conserved amino acids 91–101 and 126–137 of BAdV-3 protein VII interact with viral proteins IVa2 and VIII.

Supplementary Materials: The following supporting information can be downloaded at: https://www.mdpi.com/article/10.3390/v16050732/s1, Table S1. List of primers used for PCR [69,70]; Table S2. Other cellular proteins identified from LC-MS/MS. nd: No Data; Table S3. Ribosomal proteins identified from LC-MS/MS; Table S4. Mitochondrial proteins identified from LC-MS/MS. nd: No Data; Table S5. Cytoskeleton proteins identified from LC-MS/MS; Table S6. Nuclear proteins identified from LC-MS/MS. nd: No Data; Table S7. Nucleolar proteins identified from LC-MS/MS. nd: No Data; Table S8. Summary for 3.9 Results (For both BiFC assay & CO-IP); Table S9. Summary for 3.10 Results (For both BiFC assay & CO-IP); Table S10. The percentage of cells showing similar display of protein distribution; Table S11. The percentage of cells showing similar display of protein distribution; Table S12. The percentage of cells showing similar display of protein distribution; Figure S1. Western blots. Proteins from the lysates of cells co-transfected with indicated plasmids were separated by 12 % SDS-PAGE, transferred to nitrocellulose and probed in Western blot using (A) anti-HA MAb, B) anti-IVa2 sera. Molecular weight markers are shown on the left of the panel; Figure S2. Western blot. Proteins from the lysates of cells co-transfected with indicated plasmid DNAs separated by 12% SDS-PAGE, transferred to nitrocellulose and probed in Western blot using (A) anti-HA MAb. (B) anti-pVIII sera. Molecular weight markers are shown on the left of the panel.

Author Contributions: Conceptualization, S.K. and S.K.T.; methodology, S.K. and F.D.; formal analysis, S.K. and F.D.; investigation, S.K. and F.D.; data curation, S.K., F.D. and S.K.T.; writing—original draft preparation, S.K. and S.K.T.; writing—review and editing, S.K. and S.K.T. All authors have read and agreed to the published version of the manuscript.

Funding: The work was supported by a grant from Natural Sciences and Engineering Council of Canada to SKT. Shermila Kulanayake and Faryal Dar are partially supported by scholarships from School of Public Health, University of Saskatchewan. VIDO receives operational funding from Government of Saskatchewan through Innovation Saskatchewan and Ministry of Agriculture, and from Canada Foundation of Innovation through the major Science initiatives.

Institutional Review Board Statement: Not applicable.

Informed Consent Statement: Not applicable.

Data Availability Statement: The original contributions presented in the study are included in the article and Supplementary Materials, further inquiries can be directed to the corresponding author.

Acknowledgments: The authors are thankful to Dielle Whitecross for helping with purification of GST.Importin fusion proteins and other members of Tikoo's laboratory including Tekeleselassie A. Woldemariam, Abdelrahman Said and Li Hao for their valuable contributions. The work presented here forms part of the PhD thesis of S.K. Published as manuscript # 1047.

Conflicts of Interest: The authors have no conflicts of interest. Moreover, the funders had no role in the design of the study, in the collection, analysis or interpretation of the data, in the writing of the manuscript or in the decision to publish the results.

References

1. Reddy, P.S.; Idamakanti, N.; Zakhartchouk, A.N.; Baxi, M.K.; Lee, J.B.; Pyne, C.; Babiuk, L.A.; Tikoo, S.K. Nucleotide sequence, genome organization, and transcription map of bovine adenovirus type 3. *J. Virol.* **1998**, *72*, 1394–1402. [CrossRef] [PubMed]
2. Reddy, V.S.; Nemerow, G.R. Structures and organization of adenovirus cement proteins provide insights into the role of capsid maturation in virus entry and infection. *Proc. Natl. Acad. Sci. USA* **2014**, *111*, 11715–11720. [CrossRef] [PubMed]
3. Zhao, X.; Tikoo, S.K. Nuclear and Nucleolar localization of bovine adenovirus-3 protein V. *Front. Microbiol.* **2020**, *11*, 579593. [CrossRef] [PubMed]
4. Said, A.; Wang, W.; Woldermariam, T.; Tikoo, S.K. Domains of bovine adenovirus-3 protein 22K involved in interacting with viral protein 52K and cellular importins alpha-5/alpha-7. *Virology* **2018**, *522*, 209–219. [CrossRef] [PubMed]

5. Woldemariam, T.; Wang, W.; Said, A.; Tikoo, S.K. Regions of bovine adenovirus-3 IVa2 involved in nuclear/nucleolar localization and interaction with pV. *Virology* **2020**, *546*, 25–37. [CrossRef]
6. Wodrich, H.; Guan, T.; Cingolani, T.; Von Seggern, D.; Nemerow, G.; Gerace, L. Switch from capsid protein import to adenovirus assembly by cleavage of nuclear transport signals. *EMBO J.* **2003**, *22*, 6245–6255. [CrossRef] [PubMed]
7. Wodrich, H.; Cassany, A.; D'Angelo, M.A.; Guan, T.; Nemerow, G.; Gerace, L. Adenovirus core protein pVII is translocated into the nucleus by multiple import receptor pathways. *J. Virol.* **2006**, *80*, 9608–9618. [CrossRef] [PubMed]
8. Olson, M.O.; Dundr, M. The moving parts of the nucleolus. *Histochem. Cell Biol.* **2005**, *123*, 203–216. [CrossRef] [PubMed]
9. Mirza, M.A.; Weber, J. Structure of adenovirus chromatin. *Biochim. Biophys. Acta* **1982**, *696*, 76–86. [CrossRef]
10. Lischwe, M.A.; Sung, M.T. A histone-like protein from adenovirus chromatin. *Nature* **1977**, *267*, 552–554. [CrossRef]
11. Kulanayake, S.; Tikoo, S.K. Adenovirus Core Proteins: Structure and Function. *Viruses* **2021**, *13*, 388. [CrossRef] [PubMed]
12. Johnson, J.S.; Osheim, Y.N.; Xue, Y.; Emanuel, M.R.; Lewis, P.W.; Bankovich, A.; Beyer, A.L.; Engel, D.A. Adenovirus protein VII condenses DNA, represses transcription, and associates with transcriptional activator E1A. *J. Virol.* **2004**, *78*, 6459–6468. [CrossRef] [PubMed]
13. Puntener, D.; Engelke, M.F.; Ruzsics, Z.; Strunze, S.; Wilhelm, C.; Greber, U.F. Stepwise loss of fluorescent core protein V from human adenovirus during entry into cells. *J. Virol.* **2011**, *85*, 481–496. [CrossRef] [PubMed]
14. Ostapchuk, P.; Suomalainen, M.; Zheng, Y.; Boucke, K.; Greber, U.F.; Hearing, P. The adenovirus major core protein VII is dispensable for virion assembly but is essential for lytic infection. *PLoS Pathog.* **2017**, *13*, e1006455. [CrossRef] [PubMed]
15. Davison, A.J.; Benko, M.; Harrach, B. Genetic content and evolution of adenoviruses. *J. Gen. Virol.* **2003**, *84 Pt 11*, 2895–2908. [CrossRef] [PubMed]
16. Cheng, P.H.; Rao, X.M.; McMasters, K.M.; Zhou, H.S. Molecular basis for viral selective replication in cancer cells: Activation of CDK2 by adenovirus induced cyclin E. *PLoS ONE* **2013**, *8*, e57340. [CrossRef]
17. Makadiya, N.; Gaba, A.; Tikoo, S.K. Cleavage of bovine adenovirus type 3 non-structural 100K protein by protease is required for nuclear localization in infected cells but is not essential for virus replication. *J. Gen. Virol.* **2015**, *96*, 2749–2763. [CrossRef]
18. Stracker, T.H.; Lee, D.V.; Carson, C.T.; Araujo, F.D.; Ornelles, D.A.; Weitzman, M.D. Serotype-specific reorganization of the Mre11 complex by adenoviral E4orf3 proteins. *J. Virol.* **2005**, *79*, 6664–6673. [CrossRef]
19. Papp, Z.; Middleton, D.M.; Mittal, S.K.; Babiuk, L.A.; Baca-Estrada, M.E. Mucosal immunization with recombinant adenoviruses: Induction of immunity and protection of cotton rats against respiratory bovine herpesvirus type 1 infection. *J. Gen. Virol.* **1997**, *78*, 2933–2943. [CrossRef]
20. Du, E.; Tikoo, S.K. Efficient replication and generation of recombinant bovine adenovirus-3 in nonbovine cotton rat lung cells expressing I-SceI endonuclease. *J. Gene Med.* **2010**, *12*, 840–847. [CrossRef]
21. Anand, S.K.; Gaba, A.; Singh, J.; Tikoo, S.K. Bovine adenovirus 3 core protein precursor pVII localizes to mitochondria, and modulates ATP synthesis, mitochondrial Ca2+ and mitochondrial membrane potential. *J. Gen. Virol.* **2014**, *95 Pt 2*, 442–452. [CrossRef] [PubMed]
22. Zhou, Y.; Reddy, P.S.; Babiuk, L.A.; Tikoo, S.K. Bovine adenovirus type 3 E1B(small) protein is essential for growth in bovine fibroblast cells. *Virology* **2001**, *288*, 264–274. [CrossRef] [PubMed]
23. Ayalew, L.E.; Gaba, A.; Kumar, P.; Tikoo, S.K. Conserved regions of bovine adenovirus-3 pVIII contain functional domains involved in nuclear localization and packaging in mature infectious virions. *J. Gen. Virol.* **2014**, *95*, 1743–1754. [CrossRef] [PubMed]
24. Depping, R.; Steinhoff, A.; Schindler, S.G.; Friedrich, B.; Fagerlund, R.; Metzen, E.; Hartmann, E.; Kohler, M. Nuclear translocation of hypoxia-inducible factors (HIFs): Involvement of the classical importib α/β pathway. *Biochim. Acta* **2008**, *1783*, 394–404. [CrossRef] [PubMed]
25. Lai, M.C.; Lin, R.I.; Tarn, W.Y. Transportin-SR2 mediates nuclear import of phosphorylated SR proteins. *Proc. Nat. Acad. Sci. USA* **2001**, *98*, 10154–10159. [CrossRef] [PubMed]
26. Kulshreshtha, V.; Babiuk, L.A.; Tikoo, S.K. Role of bovine adenovirus-3 33K protein in viral replication. *Virology* **2004**, *323*, 59–69. [CrossRef] [PubMed]
27. Levin, A.; Armon-Omer, A.; Rosenbluh, J.; Melamed-Book, N.; Graessmann, A.; Waigmann, E.; Loyter, A. Inhibition of HIV-1 integrase nuclear import and replication by a peptide bearing integrase putative nuclear localization signal. *Retrovirology* **2009**, *6*, 112. [CrossRef] [PubMed]
28. Zhao, X. The Role of Bovine Adenovirus-3 Protein V (pV) in Virus Replication. Ph.D. Thesis, Department of Veterinary Microbiology, University of Saskatchewan, Saskatoon, SK, Canada, 2016.
29. Kulshreshtha, V.; Tikoo, S.K. Interaction of bovine adenovirus-3 33K protein with other viral proteins. *Virology* **2008**, *381*, 29–35. [CrossRef] [PubMed]
30. Kosugi, S.; Hasebe, M.; Tomita, M.; Yanagawa, H. Systematic identification of cell cycle-dependent yeast nucleocytoplasmic shuttling proteins by prediction of composite motifs. *Proc. Nat. Acad. Sci. USA* **2009**, *106*, 10171–10176. [CrossRef]
31. Yachdav, G.; Kloppmann, E.; Kajan, L.; Hecht, M.; Goldberg, T.; Hamp, T.; Honigschmid, P.; Schafferhans, A.; Roos, M.; Bernhofer, M.; et al. PredictProtein—An open resource for online prediction of protein structural and functional features. *Nucleic Acids Res.* **2014**, *42*, 337–343. [CrossRef]
32. Wu, Q.; Tikoo, S.K. Altered tropism of recombinant bovine adenovirus type-3 expressing chimeric fiber. *Virus Res.* **2004**, *99*, 9–15. [CrossRef]

33. Field, J.; Nikawa, J.; Broek, D.; MacDonald, B.; Rodgers, L.; Wilson, I.A.; Lerner, R.A.; Wigler, M. Purification of a RAS-responsive adenylyl cyclase complex from Saccharomyces cerevisiae by use of an epitope addition method. *Mol. Cell. Biol.* **1988**, *8*, 2159–2165.
34. Gaba, A.; Ayalew, L.; Makadiya, N.; Tikoo, S. Proteolytic Cleavage of Bovine Adenovirus 3-Encoded pVIII. *J. Virol.* **2017**, *91*, e00211-17. [CrossRef]
35. Arnberg, N. Adenovirus receptors: Implications for tropism, treatment and targeting. *Rev. Med. Virol.* **2009**, *19*, 165–178. [CrossRef]
36. Greber, U.F.; Willetts, M.; Webster, P.; Helenius, A. Stepwise dismantling of adenovirus 2 during entry into cells. *Cell* **1993**, *75*, 477–486. [CrossRef]
37. Russell, W.C. Adenoviruses: Update on structure and function. *J. Gen. Virol.* **2009**, *90*, 1–20. [CrossRef] [PubMed]
38. Vellinga, J.; Van der Heijdt, S.; Hoeben, R.C. The adenovirus capsid: Major progress in minor proteins. *J. Gen. Virol.* **2005**, *86*, 1581–1588. [CrossRef] [PubMed]
39. Weber, J.M. Adenovirus endopeptidase and its role in virus infection. *Curr. Top. Microbiol. Immunol.* **1995**, *199 Pt 1*, 227–235.
40. Dai, X.; Wu, L.; Sun, R.; Zhou, Z.H. Atomic Structures of Minor Proteins VI and VII in Human Adenovirus. *J. Virol.* **2017**, *91*, e00850-17. [CrossRef]
41. Perez-Vargas, J.; Vaughan, R.C.; Houser, C.; Hastie, K.M.; Kao, C.C.; Nemerow, G.R. Isolation and characterization of the DNA and protein binding activities of adenovirus core protein V. *J. Virol.* **2014**, *88*, 9287–9296. [CrossRef]
42. Reddy, V.S.; Barry, M.A. Structural Organization and Protein-Protein Interactions in Human Adenovirus Capsid. *Subcell. Biochem.* **2021**, *96*, 503–518. [CrossRef] [PubMed]
43. Imperiale, M.J.; Akusjnarvi, G.; Leppard, K.N. Post-Transcriptional control of adenovirus gene expression. *Curr. Top. Microbiol. Immunol.* **1995**, *199 Pt 2*, 139–171. [PubMed]
44. Karen, K.A.; Hearing, P. Adenovirus core protein VII protects the viral genome from a DNA damage response at early times after infection. *J. Virol.* **2011**, *85*, 4135–4142. [CrossRef] [PubMed]
45. Weber, J. Genetic analysis of adenovirus type 2 III. Temperature sensitivity of processing viral proteins. *J. Virol.* **1976**, *17*, 462–471. [CrossRef] [PubMed]
46. Mangel, W.F.; San Martin, C. Structure, function and dynamics in adenovirus maturation. *Viruses* **2014**, *6*, 4536–4570. [CrossRef] [PubMed]
47. Nemerow, G.R.; Stewart, P.L.; Reddy, V.S. Structure of human adenovirus. *Curr. Opin. Virol.* **2012**, *2*, 115–121. [CrossRef]
48. Boudin, M.L.; D'Halluin, J.C.; Cousin, C.; Boulanger, P. Human adenovirus type 2 protein IIIa. II. Maturation and encapsidation. *Virology* **1980**, *101*, 144–156. [CrossRef] [PubMed]
49. Zhang, W.; Arcos, R. Interaction of the adenovirus major core protein precursor, pVII, with the viral DNA packaging machinery. *Virology* **2005**, *334*, 194–202. [CrossRef]
50. Cheng, L.; Huang, X.; Li, X.; Xiong, W. Cryo-EM structures of two bovine adenovirus type 3 intermediates. *Virology* **2014**, *450–451*, 174–181. [CrossRef]
51. Gallardo, J.; Pérez-Illana, M.; Martín-González, N.; San Martín, C. Adenovirus structure: What is new? *Int. J. Mol. Sci.* **2021**, *22*, 5240. [CrossRef]
52. Hackenbrack, N.; Rogers, M.B.; Ashley, R.E.; Keel, M.K.; Kubiski, S.V.; Bryan, J.A.; Ghedin, E.; Holmes, E.C.; Hafenstein, S.L.; Allison, A.B. Evolution and cryo-electron microscopy capsid structure of a North-American bat adenovirus and its relationship to other mastadenoviruses. *J. Virol.* **2017**, *91*, e01504-16. [CrossRef] [PubMed]
53. Marabini, R.; Condezo, G.N.; Krupovic, M.; Menendez-Conejero, R.; Gomez-Blanco, J.; San, M.C. Near-atomic structure of an atadenovirus reveals a conserved capsid-binding motif and intergenera variations in cementing proteins. *Sci. Adv.* **2021**, *7*, eabe6008. [CrossRef] [PubMed]
54. Lange, A.; Mills, R.E.; Lange, C.J.; Stewart, M.; Devine, S.E.; Corbett, A.H. Classical nuclear localization signals: Definition, function, and interaction with importin alpha. *J. Biol. Chem.* **2007**, *282*, 5101–5105. [CrossRef] [PubMed]
55. Christophe, D.; Christophe-Hobertus, C.; Pichon, B. Nuclear targeting of proteins: How many different signals? *Cell Signal* **2000**, *12*, 337–341. [CrossRef] [PubMed]
56. Schaley, J.E.; Polonskaia, M.; Hearing, P. The Adenovirus E4-6/7 Protein Directs Nuclear Localization of E2F-4 via an Arginine-Rich Motif. *J. Virol.* **2005**, *79*, 2301–2308. [CrossRef] [PubMed]
57. Al-Wassiti, H.A.; Thomas, D.R.; Wagstaff, K.M.; Fabb, S.A.; Jans, D.A.; Johnston, A.P. Adenovirus Terminal Protein Contains a Bipartite Nuclear Localisation Signal Essential for Its Import into the Nucleus. *Int. J. Mol. Sci.* **2021**, *22*, 3310. [CrossRef] [PubMed]
58. Paterson, C.P.; Ayalew, L.E.; Tikoo, S.K. Mapping of nuclear import signal and importin alpha3 binding regions of 52K protein of bovine adenovirus-3. *Virology* **2012**, *432*, 63–72. [CrossRef] [PubMed]
59. Kulshreshtha, V.; Ayalew, L.E.; Islam, A.; Tikoo, S.K. Conserved arginines of bovine adenovirus-3 33K protein are important for transportin-3 mediated transport and virus replication. *PLoS ONE* **2014**, *9*, e101216. [CrossRef] [PubMed]
60. Reed, M.L.; Dove, B.K.; Jackson, R.M.; Collins, R.; Brooks, G.; Hiscox, J.A. Delineation and modelling of a nucleolar retention signal in the coronavirus nucleocapsid protein. *Traffic* **2006**, *7*, 833–848. [CrossRef]
61. Cheng, G.; Brett, M.E.; He, B. Signals that dictate nuclear, nucleolar, and cytoplasmic shuttling of the gamma (1)34.5 protein of herpes simplex virus type 1. *J. Virol.* **2002**, *76*, 9434–9445. [CrossRef]
62. Cros, J.F.; Garcia-Sastre, A.; Palese, P. An unconventional NLS is critical for the nuclear import of the influenza A virus nucleoprotein and ribonucleoprotein. *Traffic* **2005**, *6*, 205–213. [CrossRef] [PubMed]

63. Zhang, W.; Imperiale, M.J. Requirement of the adenovirus IVa2 protein for virus assembly. *J. Virol.* **2003**, *77*, 3586–3594. [CrossRef] [PubMed]
64. Martin-Gonzalez, N.; Hernando-Perez, M.; Condezo, G.N.; Perez-Illana, M.; Siber, A.; Reguera, D.; Ostapchuk, P.; Hearing, P.; San Martin, C.; de Pablo, P.J. Adenovirus major core protein condenses DNA in clusters and bundles, modulating genome release and capsid internal pressure. *Nucleic Acids Res.* **2019**, *47*, 9231–9242. [CrossRef] [PubMed]
65. Perez-Berna, A.J.; Marion, S.; Chichon, F.J.; Fernandez, J.J.; Winkler, D.C.; Carrascosa, J.L.; Steven, A.C.; Siber, A.; San Martin, C. Distribution of DNA-condensing protein complexes in the adenovirus core. *Nucleic Acids Res.* **2015**, *43*, 4274–4283. [CrossRef] [PubMed]
66. Rohn, K.; Prusas, C.; Monreal, G.; Hess, M. Identification and characterization of penton base and pVIII protein of egg drop syndrome virus. *Virus Res.* **1997**, *47*, 59–65. [CrossRef] [PubMed]
67. Hernando-Perez, M.; Martin-Gonzalez, N.; Perez-Illana, M.; Suomalainen, M.; Condezo, G.N.; Ostapchuk, P.; Gallardo, J.; Menendez, M.; Greber, U.F.; Hearing, P.; et al. Dynamic competition for hexon binding between core protein VII and lytic protein VI promotes adenovirus maturation and entry. *Proc. Natl. Acad. Sci. USA* **2020**, *117*, 13699–13707. [CrossRef] [PubMed]
68. Liu, G.Q.; Babiss, L.E.; Volkert, F.C.; Young, C.S.; Ginsberg, H.S. A thermolabile mutant of adenovirus 5 resulting from a substitution mutation in the protein VIII gene. *J. Virol.* **1985**, *53*, 920–925. [CrossRef] [PubMed]
69. Taylor, L.A.; Rose, R.E. A correction in the nucleotide sequence of the Tn903 kanamycin resistance determinant in pUC4K. *Nucleic Acids Res* **1988**, *16*, 358. [CrossRef]
70. Zakhartchouk, A.; Connors, W.; Van Kessel, A.; Tikoo, S.K. Bovine adenovirus type 3 containing heterologous protein in the C-terminus of minor capsid protein IX. *Virology* **2004**, *320*, 291–300. [CrossRef]